



Improving thoracic malignancy re-irradiation outcomes: preventing radiation-induced toxicity using stereotactic body radiotherapy with radioprotector agents

Meridith L. Balbach¹, Bailey A. Nelson¹, and Neal E. Dunlap, M.D.¹
 Department of Radiation Oncology, James Graham Brown Cancer Center¹
 University of Louisville School of Medicine

Introduction

Primary lung cancer is the leading cause of cancer deaths in both men and women in the United States; moreover, the lung is the most common site for metastases of multiple different cancers. At initial presentation, approximately 61% of non-small cell lung cancer (NSCLC) patients will receive radiation therapy (RT). Radiation kills cancer cells by damaging DNA with free radicals and double-stranded breaks (Fig. 1).

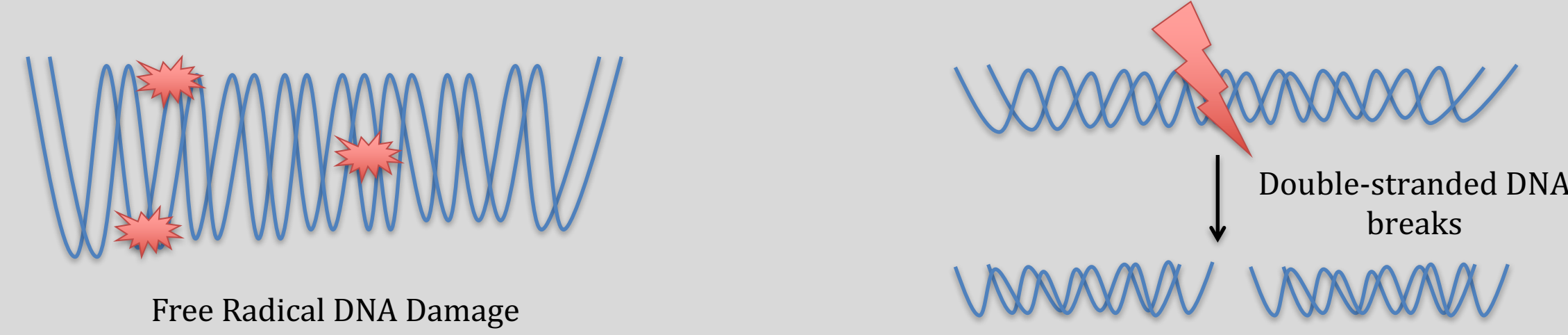


Fig. 1: Radiation-induced double-stranded DNA breaks and free radicals are detrimental to cancer cells.

Despite high loco-regional failure rates, recurrent thoracic malignancy patients previously treated with radiotherapy have limited therapeutic options, as second-line systemic chemotherapy response rates are poor and surgical resection is infeasible due to fibrosis induced by prior radiation. However, re-irradiation to recurrent thoracic malignancies, metastatic lesions, and new lung primaries using stereotactic body radiotherapy (SBRT), a technique enabling delivery of high biologically effective doses with minimal damage to surrounding tissues, has resulted in high in-field local tumor control and lower toxicity relative to conventional external beam radiotherapy (EBRT) (Fig. 2).

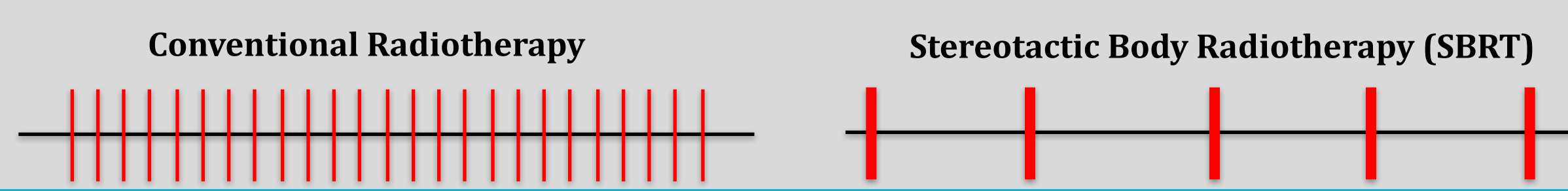


Fig. 2: This image demonstrates differences in fractionation schedules with conventional RT (like EBRT) and SBRT. Each red line represents one radiation dose, with a larger width indicating a larger dose.

Although toxicity is lower, rates of severe (grade ≥ 3) pneumonitis have been reported to be as high as 30%. The use of radioprotector agents has the potential to further reduce this toxicity in re-irradiation patients. Pentoxifylline (PTX), a xanthine derivative hypothesized to ameliorate lung injury through indirect inhibition of pro-inflammatory molecule production (Fig. 3), is one such radioprotector agent. Prior studies have demonstrated that delayed administration of pentoxifylline and Vitamin E to former malignancy patients with radiation-induced fibrosis results in significant fibrotic tissue regression and improvement of radiation-induced physical impairment.

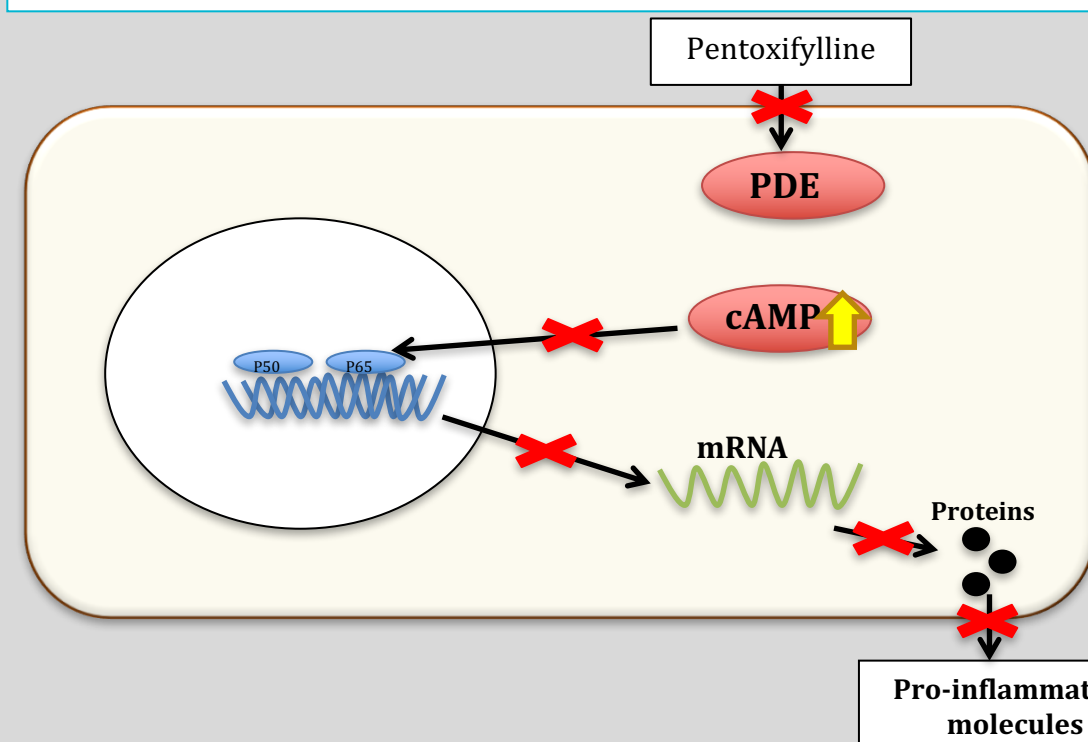


Fig. 3: Pentoxifylline is a competitive non-selective PDE inhibitor, which increases intracellular levels of cAMP and inhibits tumor necrosis factor (TNF) and leukotriene synthesis downstream. Thus, Pentoxifylline decreases inflammation.

Objective

Following a recent breast cancer study demonstrating that combined administration of pentoxifylline and Vitamin E following radiation therapy results in lower rates of breast fibrosis, this non-randomized study aims to prospectively evaluate SBRT delivery with administration of pentoxifylline and Vitamin E prior to, during, and following therapy in the setting of previous thoracic irradiation. A recent re-treatment series with a similar dosing schedule by Kelly et. al estimated \geq grade 3 pulmonary and esophageal toxicity to be approximately 30%. Our goal is to reduce \geq grade 3 pulmonary and esophageal toxicity to 15%.

Methods

51 patients were enrolled with recurrent or new primary thoracic malignancies after a previous histologically proven thoracic malignancy treated with radiation therapy with or without chemotherapy. Pathologic confirmation of a new or recurrent tumor was suggested but not required.

Eligible Patients

- ≥ 18 yo with ECOG 0-1
- Prior thoracic malignancy treated with EBRT with or without systemic chemotherapy
- New or loco-regional recurrent lung malignancy
- Negative serum pregnancy test and medically effective means of birth control if sexually active
- Provided informed consent
- Exclusion: overlapping systemic chemotherapy or chemotherapy within 4 weeks of initiation of SBRT

Baseline Function

- Diagnostic Chest CT
- FDG-PET
- 4D Simulation CT scan
- QOL assessment
- PFTs
 - Exclusion criteria: FEV1 $<$ 20% predicted and/or DLCO $<$ 20% predicted

SBRT

- 50 Gy in 5 fx
- 1 week prior to RT \rightarrow 12 weeks after completion of RT
 - Vitamin E 400 IU qd
 - Pentoxifylline 400 mg tid

Follow-Up

- Toxicity analysis q 3 mo (Fig. 5)
- PFTs with DLCO at 6 mo post SBRT and yearly
- CT 8-12 wks post-radiation, then q3 mo for 2 years post-treatment
- FDG-PET 6 mo post-SBRT
- Tumor Response (Fig. 6)

Fig. 4: CTEP Common Terminology Criteria for Adverse Events (CTCAE v4.0)

Adverse Event	Grade				
	1	2	3	4	5
Pneumonitis	Asymptomatic; clinical or diagnostic observations only; intervention not indicated	Symptomatic; medial intervention indicated; limiting instrumental ADL	Severe symptoms; limiting self care ADL; oxygen indicated	Life-threatening respiratory compromise; urgent intervention indicated	Death
Esophagitis	Asymptomatic; clinical or diagnostic observations only; intervention not indicated	Symptomatic; altered eating/swallowing; oral supplements indicated	Severely altered eating/swallowing; tube feeding; TPN or hospitalization indicated	Life-threatening consequences; urgent operative intervention indicated	Death

Tumor Response	Radiologic Measurements
Complete Response (CR)	Disappearance of all target lesions
Partial Response (PR)	$>$ 30% decrease in sum of LD of target lesions
Stable Disease (SD)	Does not qualify as PR or PD
Progressive Disease (PD)	$>$ 20% increase in sum of LD of target lesions

Fig. 5: Patients were assigned a tumor response grade based on a modified version of the RECIST criteria guidelines. *LD = Longest Diameter

Results

Characteristic	Number	Percent
Sex		
Female	12	44.4%
Male	15	55.6%
Age		
40-50 yo	2	7.4%
51-60 yo	5	18.5%
61-70 yo	7	25.9%
71-80 yo	10	37.0%
81-90 yo	3	11.1%
Smoking		
Current	11	40.7%
Non-smoker		
Former	14	51.9%
Never	2	7.4%
Tumor Type		
New	5	18.5%
Recurrent	20	74.1%
Persistent	2	7.4%
Risk for Toxicity (n=20)		
Low	9	45%
High	11	55%

Fig. 6: Patient and tumor characteristics. We report on the initial cohort of 27 patients with a minimum of 1 year follow-up. Ninety-six percent of patients completed the study drugs as directed. One patient reduced the dose of PTX to twice daily due to GI issues. Tumors were classified as recurrent, new or persistent based on radiographic imaging, pathology, and clinical presentation. Previous treatment plans for stratification into high or low risk were available for 20 patients.

	Median	Range
Previous RT dose (Gy)	54.0 Gy (n=26)	45.0 – 75.0 Gy (n=26)
Current RT PTV (cm ³)	19.5 cm ³	2.8 – 577.1 cm ³
Interval from prior RT (mo)	15 mo	1.5 – 72 mo
Re-irradiation RT dose (Gy)	50 Gy	50 Gy
Re-irradiation no. of fx	5	5

Fig. 7: Prior radiotherapy and re-irradiation characteristics. Prior radiation dose to the chest was evaluable for 26 patients. Re-irradiation interval was defined as the time from completion of initial chest radiation and initiation of re-irradiation.

Toxicity (n=26)*	Grade	Number	Percent
Pneumonitis	I	4	15.3%
	II	5	19.2%
	III	1	3.8%
	IV-V	0	0%
Esophagitis	I	5	19.2%
	II-V	0	0%
Chest Wall Pain	I	1	3.8%
	II	2	7.6%
	III	1	3.8%
	IV-V	0	0%
Dyspnea	I	4	15.3%
	II	5	19.2%
	III	1	3.8%
	IV-V	0	0%

Fig. 8: Toxic adverse effects experienced with re-irradiation. We report on toxic side effects for 26 patients. The overall rate of symptomatic pneumonitis (grade ≥ 2) was 22%. Severe pneumonitis (grade ≥ 3) was reported in 4%. No patients experienced symptomatic esophagitis (grade ≥ 2).

Results (continued)

PFT (n=12)	Average Reduction following RT	Reduction Range following RT
FEV ₁ (n=12)	8%	0-31%
FVC (n=11)	4%	0-25%
DLCO (n=10)	9%	0-46%

Fig. 9: Pulmonary toxicity evaluation via Pulmonary Function Tests (PFTs). Available PFTs were analyzed for pulmonary toxicity. No patients developed severe pneumonitis based on PFT criteria.

Tumor Response	Number	Percent
Local control		
Complete Response	11	40.7%
Partial Response	4	14.8%
Stable Disease	2	7.4%
Progressive Disease		
Local	10	37.0%
Peripheral	5	18.5%

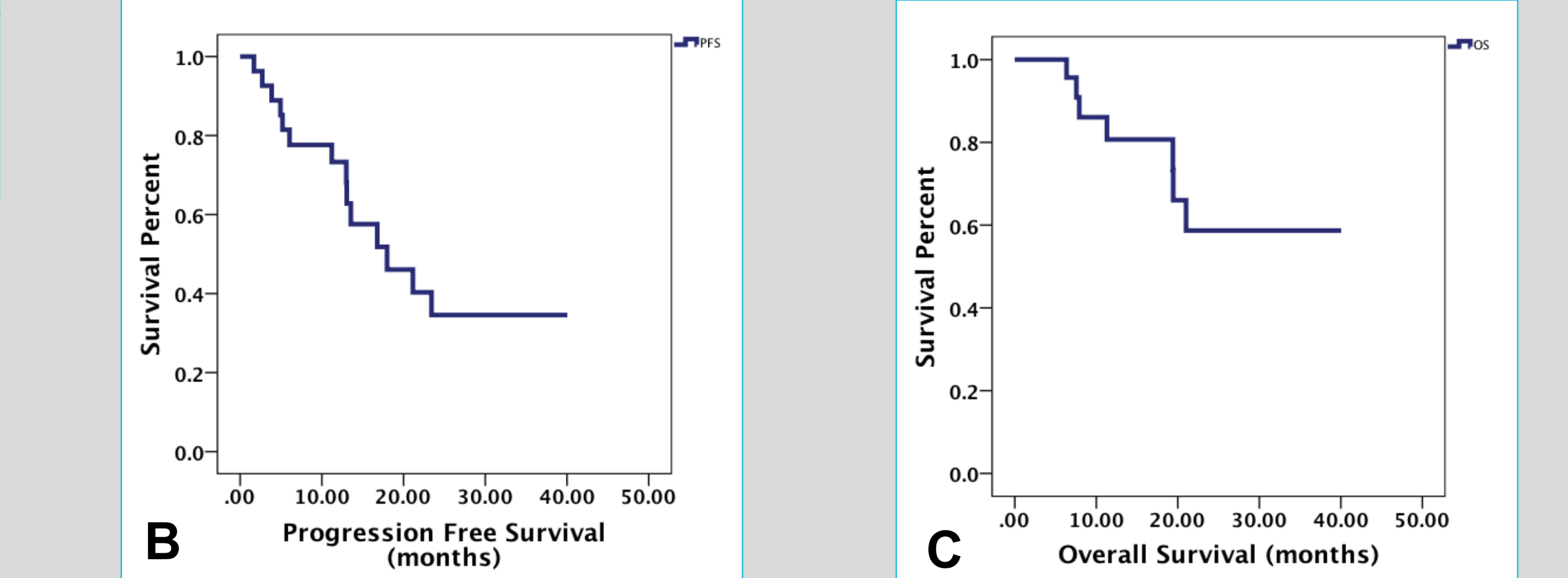


Fig. 10: Patient tumor responses (A), progression free survival (B), and overall survival (C). The estimated rate of local failure, 1 year progression free survival (PFS), and 1 year overall survival (OS) for the cohort was 37%, 66%, and 85%, respectively. Cox proportional hazard model showed significant factors for progression of increasing PTV volume (HR 1.004, 95% CI 1.001 – 1.007). Age was a predictor for increased risk of death (HR .858, 95% CI .758 - .973).

Conclusion

The initial cohort of patients shows promise for the addition of PTX and Vitamin E to SBRT in the setting of retreatment after previous thoracic radiation in reducing grade ≥ 3 pneumonitis and esophagitis.

Future Directions

- A complete analysis of the prospective clinical trial data should be performed, including:
 - Evaluation of toxicity outcomes for high vs. low risk patients as defined by prior irradiation PTV
 - Evaluation of toxicity outcomes for patients with varying time intervals between initial RT and re-irradiation
- A randomized study comparing toxicity outcomes in patients given placebo versus PTX + Vitamin E treatment
- A randomized study comparing toxicity outcomes of patients administered study drugs immediately following re-irradiation versus prior to, during, and following RT

Acknowledgements

The R25 program and this research is supported by funding from the National Cancer Institute through the R25-CA134283 grant. We appreciate the support of the James Graham Brown Cancer Center and University of Louisville School of Medicine.



Can machine learning identify patients at risk for adverse drug events using a specific medication?

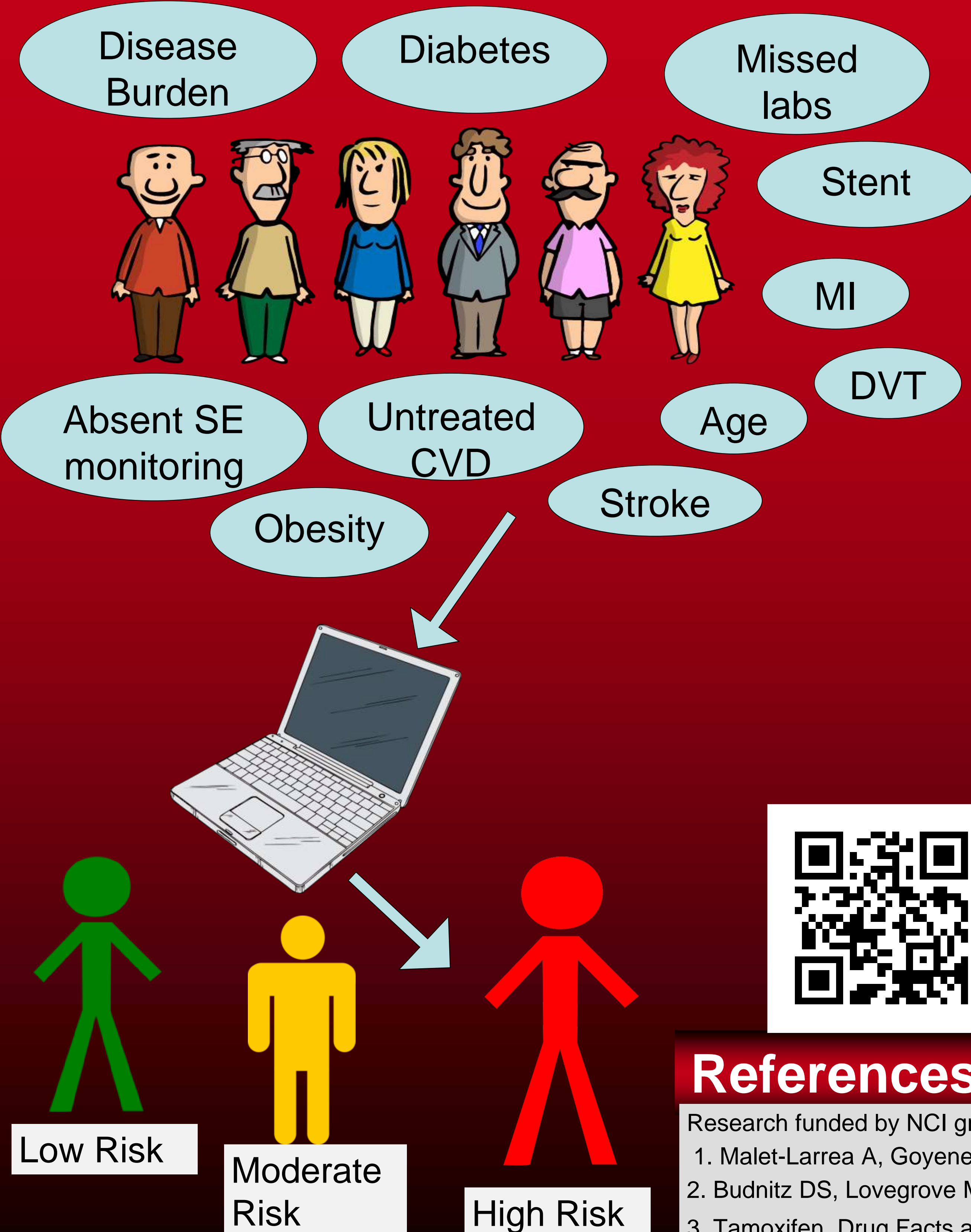
William S. Berry; Demetra Antimisiaris, PharmD, BCGP, FASCP, Department of Pharmacology and Toxicology, University of Louisville School of Medicine

Introduction

•Adverse drug events (ADEs) overall account for a high percentage of hospitalizations of older adults and it is estimated that up to 33 percent of them are due to medication related problems. [1] One way of preventing ADEs is through adequate monitoring and pharmacovigilance.[2] With the aging of our population, long term use in medically complex patients is becoming more the rule than exception, however, there is a lack of evidence describing the risks and heightened pharmacovigilance necessary to utilize medications safely in older adults. We do however have insight into what constitutes a high-risk patient from decades of Tamoxifen and pharmacovigilance reporting. [3]

Hypothesis

Machine learning can utilize data from a retrospective case series data set of 93 subjects receiving Tamoxifen to identify those at high risk of ADEs. (Fig. 1 below)



Methods

We used a set of case series pharmacovigilance data for tamoxifen to determine risk categories to use in a program called Multifactor Dimensionality Reduction (MDR). A set of 10 categories were identified as risk factors. The Data set included subjects 60 years of age and older using Tamoxifen.

We grouped multiple risk factors in several categories with the idea of working backwards to create a minimal yet robust set of criteria for analysis. This included binary encoding of each variable set into the format needed by the software. There were 10 final subcategories used to perform the analysis, a list of which you can find in the QR code, which explains what went into each category. Some of the more important ones were Diabetes, Obesity, and Age.

After we created this encoding system it underwent many iterations until we built a functioning model using MDR software. The way the software completes this task is by creating a set of imaginary groups using something called a seed, which groups categories arbitrarily thousands of times, and then reduces them into binary values and checked for correctness. The program outputs information including how well the software trained itself, how accurate each category was at defining the case state, and other useful information including graphics of various types. Generally speaking this cross value test process is indicative of useful results above 7/10 tests, and by nature only one seed tested has to achieve a score this high. Thus, random seeding machine learning may be a valid method of identifying individual medication use risk.

You can scan the QR code found on this poster for detailed information and Graphs

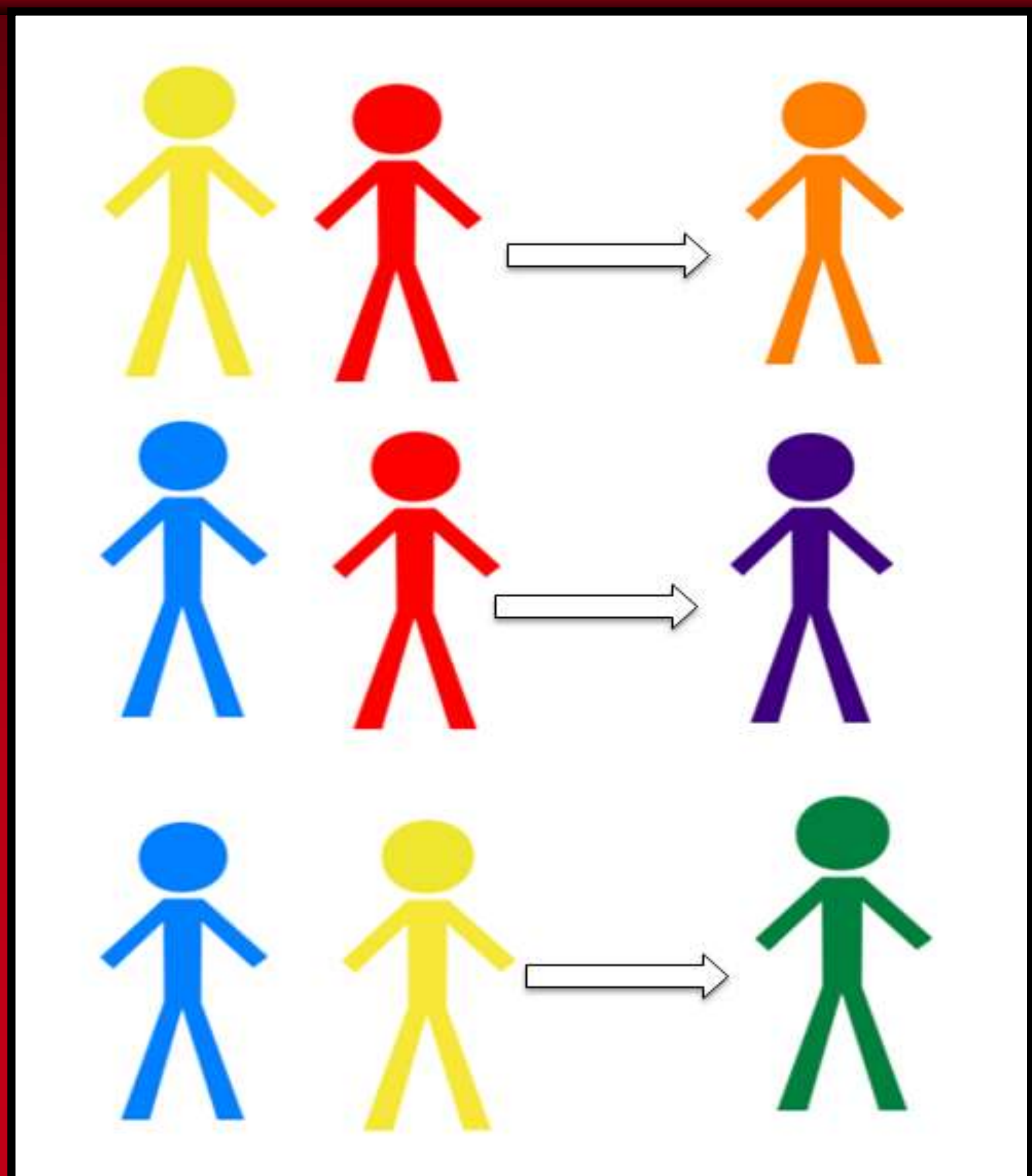


Figure 2: Primary colors= single risk factors randomly grouped and reduced into secondary colors which are assigned a risk factor and cross value by our model.

MDR works by taking multiple categories of data and reducing them into smaller categories. It does this at random based on a seed and compares the results to a case state, checking its work, and deciding whether or not what its learned is relevant compared to other results as well as the other new categories *and* the old categories.

It can also determine networked connections, and display whether or not certain categories are related even if they are not the best indication. This results in unique and useful information for pharmacovigilance and other studies, and paves the way for innovation with the application of machine learning applied to pharmacovigilance.

Results

Top Models	Bal. Acc.	Cv Training	Bal. Acc. Cv Testing	Cv Consistency
Disease Burden	0.5788		0.5788	10/10
Diabetes, Disease Burden	0.6148		0.5518	7/10
Diabetes, Disease Burden, Muscle pain	0.639		0.5729	7/10
Seed# 0 (default)				
Top Models	Bal. Acc.	Cv Training	Bal. Acc. Cv Testing	Cv Consistency
Disease Burden	0.5788		0.5788	10/10
Diabetes, Disease Burden	0.6137		0.5509	7/10
Diabetes, Disease Burden, Muscle pain	0.6392		0.5563	5/10
Seed# 8675309				
Top Models	Bal. Acc.	Cv Training	Bal. Acc. Cv Testing	Cv Consistency
Disease Burden	0.5788		0.5788	10/10
Diabetes, Disease Burden	0.6127		0.5711	8/10
Diabetes, Disease Burden, Muscle pain	0.6386		0.5755	7/10
Seed# 9000				
Top Models	Bal. Acc.	Cv Training	Bal. Acc. Cv Testing	Cv Consistency
Disease Burden	0.5788		0.5788	10/10
Diabetes, Disease Burden	0.6158		0.496	5/10
Diabetes, Disease Burden, Muscle pain	0.6417		0.4876	4/10
Seed# 270				
Top Models	Bal. Acc.	Cv Training	Bal. Acc. Cv Testing	Cv Consistency
Disease Burden	0.5792		0.5352	9/10
Diabetes, Disease Burden	0.6158		0.5178	6/10
Diabetes, Disease Burden, Muscle pain	0.641		0.546	6/10
Seed# 2				

7/10 cross value tests endorsed -[disease burden muscle pain and diabetes] and 10/10 -[disease burden]

Discussion

This study found, using MDR software, that several factors contribute to individual risk identification. The single greatest factor was “disease burden.”, or the number of comorbidities. Persons with higher comorbidity burden are more at risk for adverse events when receiving Tamoxifen. This finding aligns with clinical expert opinion and medical literature regarding canonical principles of geriatric medicine (i.e. the more medically complex the higher at risk for poor outcomes.)

We also found that cardiovascular disease and obesity were co-morbidities linked to heightened risk of ADEs with Tamoxifen use. This finding also is expected since

Conclusion

Machine learning may be a means of making use of data from a retrospective individual case study series to combine data and model risk of tamoxifen use for the individual.

This method can help identify patients at high risk of adverse outcomes to provide more individualized, efficient and appropriate pharmacovigilance. We have explored the use of MDR software to create a model for Tamoxifen use risk assessment using retrospective medical chart data. The next step is to validate the model robustly and test the method for proof of concept on other medications. This method can potentially result in lower rates of ADEs and avoidance of unnecessary hospitalization due to medication misadventure by identifying patients who need heightened surveillance and monitoring.

References and Acknowledgements

Research funded by NCI grant NCI R25-CA134283; the R25 Cancer Education Program at the University of Louisville.

1. Malet-Larrea A, Goyenechea E, Garcia-Cardenas V, et al. The impact of a medication review with follow-up service on hospital admissions in aged polypharmacy patients. Br J Clin Pharmacol 2016;82:831-8.
2. Budnitz DS, Lovegrove MC, Crosby AE. Emergency department visits for overdoses of acetaminophen-containing products. Am J Prev Med 2011;40:585-92.
3. Tamoxifen. Drug Facts and Comparisons. Fact & Comparisons [online database]. St. Louis, MO: Wolters Kluwer Health, Inc; 2011. Accessed May 8, 2017.

INTRODUCTION

Ras is an oncogene that encompasses a family of related GTPases that are involved in growth signaling. In their GTP-bound active state, Ras proteins activate several effectors that stimulate phosphorylation cascade pathways such as the MAPK pathway and the AKT pathway. Thus, activation of Ras leads to an increase in growth and survival gene expression resulting in increased cell proliferation. In human cancer, Ras is the most frequently mutated oncogene. Mutant Ras becomes locked in the active state resulting in constitutive stimulation of downstream pathways.

While Ras has been known to be involved in growth pathways, it has been also been implicated in pro-apoptotic signaling. The Ras-association domain family (RAS) is a class of Ras Death effector proteins that modulate tumor suppression activities of Ras. RASSF1A is the best studied member. It is important to study RASSF1A because the mechanisms by which RASSF1A mediates tumor suppression are not fully characterized, and RASSF1A is often transcriptionally silenced in tumors, most commonly due to promoter hyper-methylation.

In addition to dynamic regulation of protein phosphorylation, dynamic modulation of protein acetylation is also used by the cell to control protein activity. Here we discovered a novel Ras-regulated protein-protein interaction between RASSF1A and the protein acetyl transferase PCAF. Furthermore, we have identified a potential new biological mechanism by which RASSF1A mediates tumor suppression. We show that PCAF and RASSF1A form a Ras-regulated protein complex and that this interaction regulates the PCAF-mediated acetylation and activation of the key oncogenic protein β -catenin. These results are the first demonstration of a mechanism whereby Ras may modulate protein activity by modifying lysine acetylation in downstream targets.

1

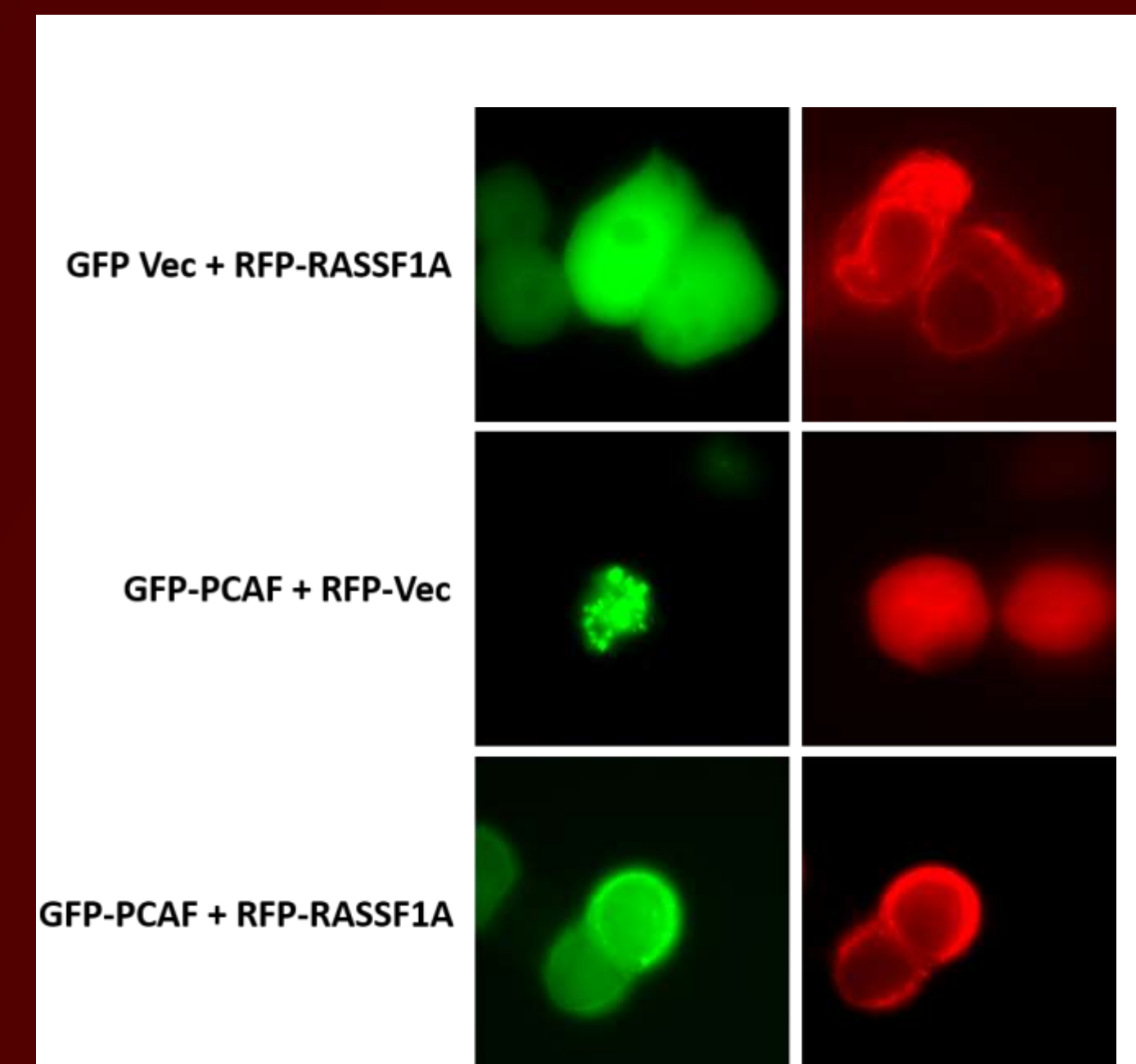


Figure 1: RASSF1A and PCAF Co-Localize in Human Cells. Expression constructs expressing GFP, GFP-PCAF, RFP, and RFP-RASSF1A were co-transfected into HEK-293T cells and incubated for 24 hours. In the control transfections, neither RASSF1A or PCAF co-localize with their respective vector controls. However, we detected a marked and distinct co-localization when PCAF and RASSF1A were co-expressed. Intriguingly, this co-localization was detected in the cytoplasm on microtubules, and the presence of RASSF1A significantly reduced the number of observed PCAF nuclear speckles.

2

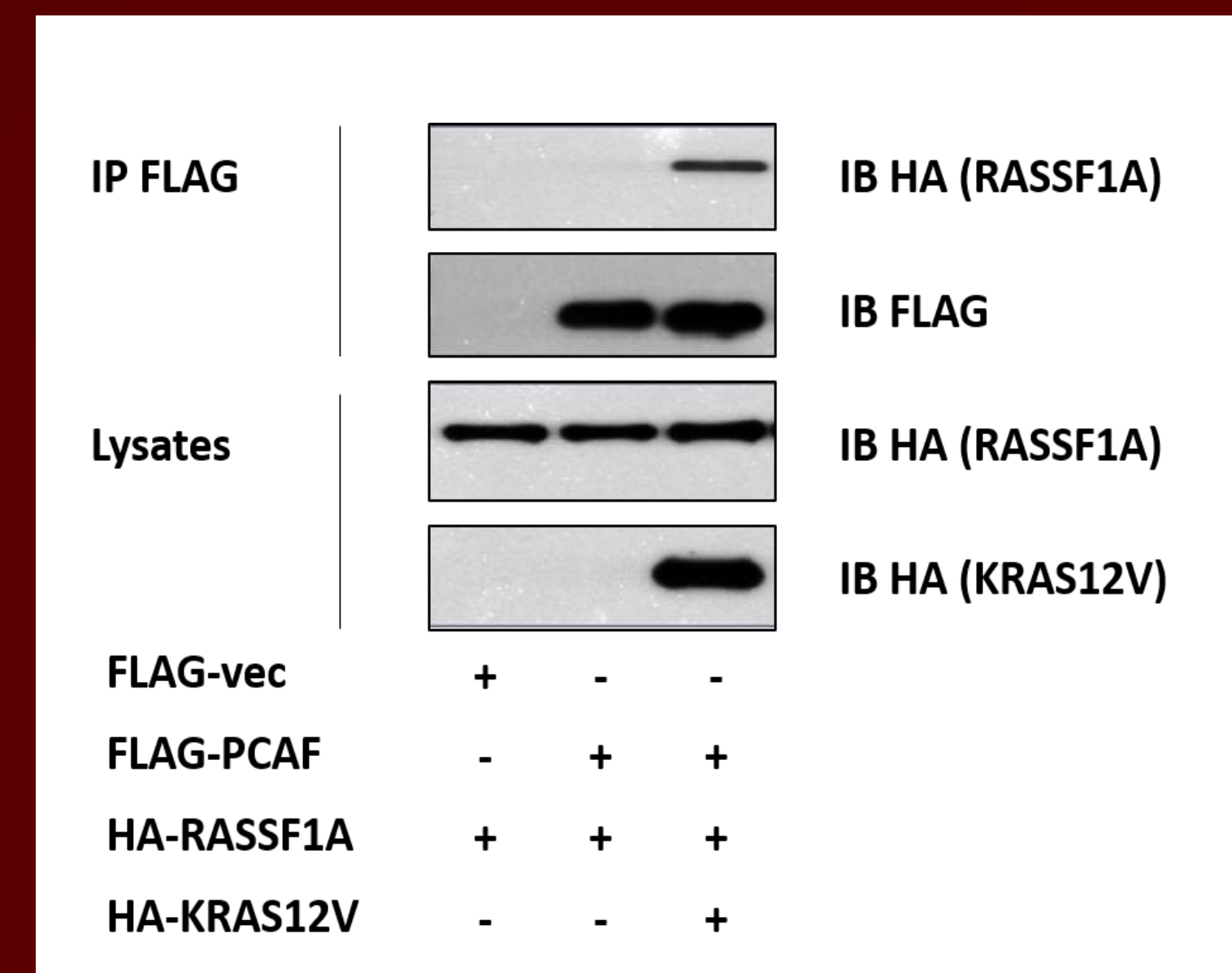


Figure 2: RASSF1A and PCAF form a Ras regulated complex. HEK293T cells were co-transfected with expression constructs coding for HA-RASSF1A, FLAG-PCAF, and HA-KRAS12V and then co-immunoprecipitated. Results showed that a protein complex was formed between RASSF1A and PCAF, and that this interaction was regulated by K-RAS (12V).

3

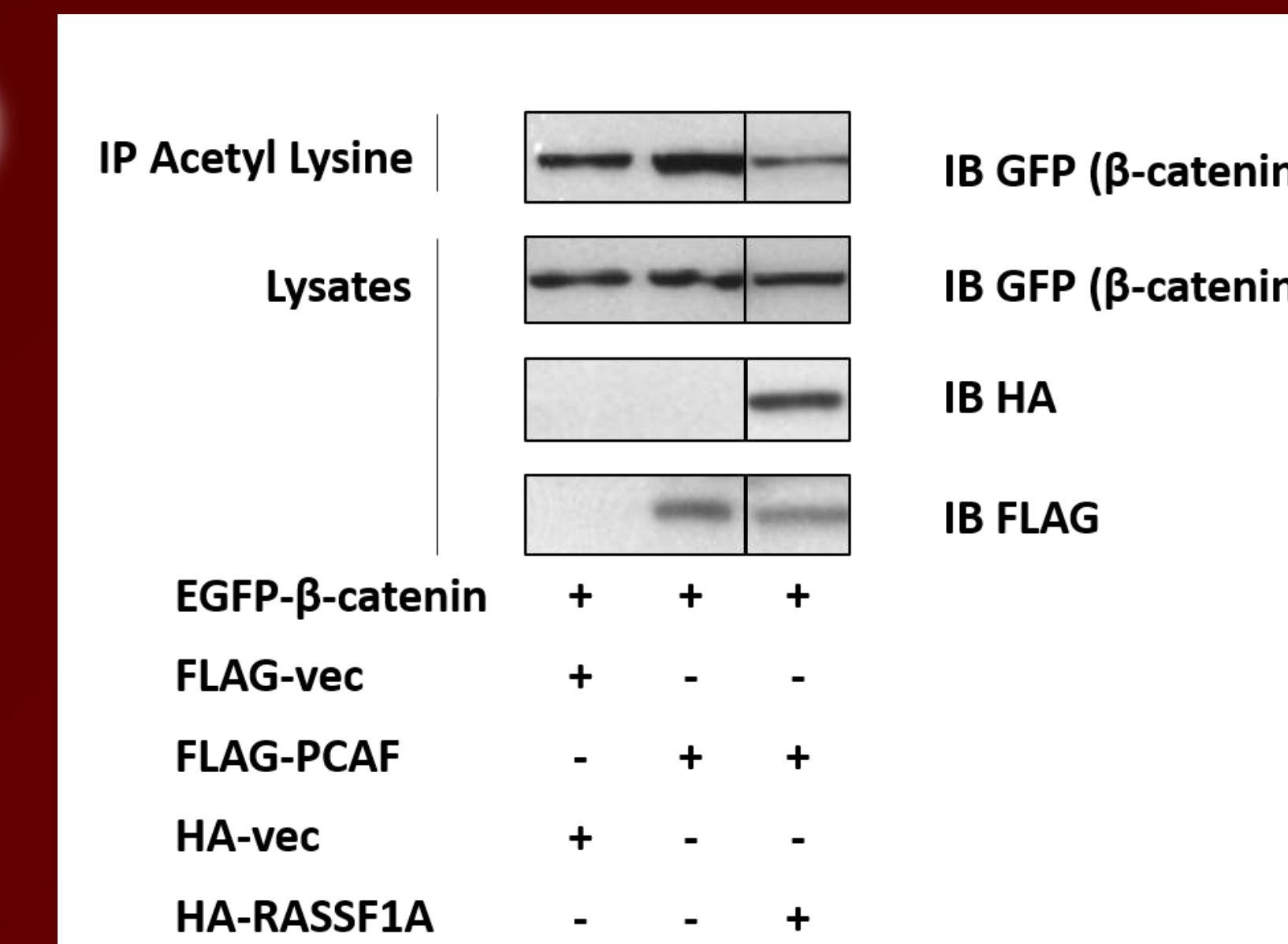


Figure 3: RASSF1A suppresses the PCAF-mediated acetylation of β -catenin. HEK-293T cells were transfected with expression constructs coding for RASSF1A, PCAF, and β -catenin. Immunoprecipitations against acetylated lysines of β -catenin were performed. Analysis of protein expression via Western blotting showed that PCAF acetylates β -catenin. However, the interaction between RASSF1A and PCAF impairs PCAF activity on β -catenin.

4

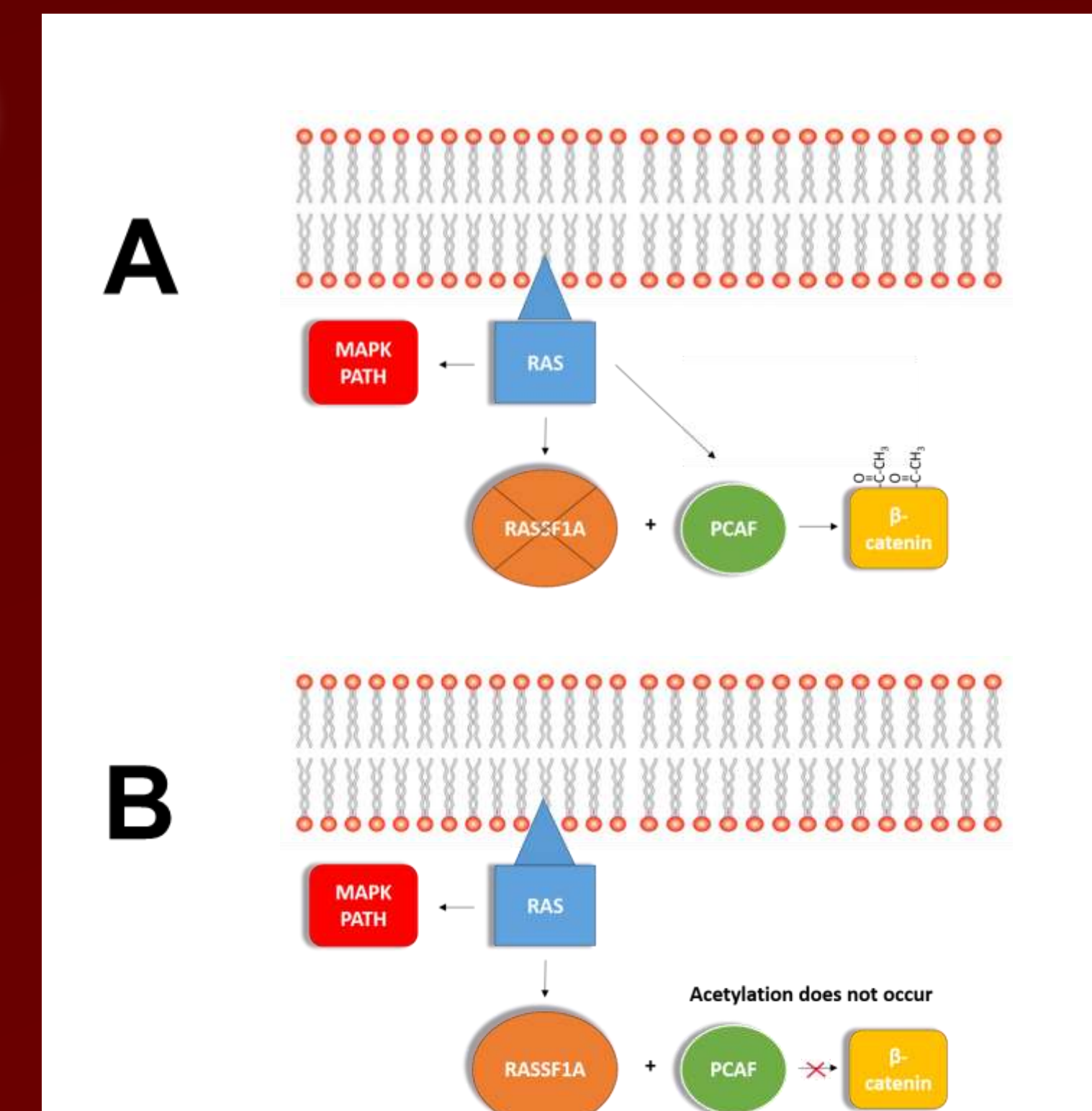


Figure 4: (A) Schematic depiction showing that in the absence of RASSF1A, Ras can function directly to PCAF. The activation of β -catenin occurs because of aberrant acetylation activity of PCAF. (B) Schematic depiction showing that RASSF1A regulates the PCAF-mediated acetylation and activation of this oncogenic substrate.

METHODS

Transformation: 1 μ g of DNA plasmid constructs were transfected into sub-cloning efficiency, chemically competent DH5 α bacteria. These plasmids contained specific ampicillin resistance markers that later allowed for the selection of bacteria when treated with antibiotics.

Miniprep: Plasmids were harvested from bacteria using a Qiagen Spin Mini-Prep Kit manufacturer's Miniprep protocol.

Cell Lines: HEK-293T cells were maintained in DMEM medium supplemented with 10% FBS and 1% penicillin-streptomycin in an incubator at 37 $^{\circ}$ C in 5% CO₂.

Transfections: HEK-293T cells were transfected with 1 μ g total mass of each expression construct coding for FLAG-vector, HA-RASSF1A, and FLAG-PCAF, with +/- PCGKRAS12V, using Jet Prime transfection reagents according to the manufacturer's protocol. In the IP against acetylated lysines of β -catenin, additional expression constructs for pEGFP- β -catenin were used. Transfected cells were left to incubate for 24 hours.

Protein Analysis: Transfected cells were lysed with a modified RIPA buffer containing 1% NP40 and protein expression of purified lysates were quantified using Bio-Rad BCA protein dye.

Immunoprecipitation: Immunoprecipitations were performed against FLAG epitope tags using FLAG-M2 conjugated agarose gel beads with equal amounts of lysates. Lysates were incubated overnight on rotator at 4 $^{\circ}$ C. Aliquots of cell lysates were saved and stored at -20 $^{\circ}$ C to be used as loading controls.

Western blotting: Samples were loaded and ran on a 4-12% Bis-Tris acrylamide gel, transferred on to a 0.2 μ M membrane, and blocked with a 5% milk and 1X TBST solution. Membranes were then immunoblotted for HA-tags using anti-HA antibodies, GFP-tags using anti-GFP antibodies, and FLAG-tags using anti-FLAG antibodies. Secondary mouse antibodies were used to probe for mouse epitope tags. Membranes were then developed with West-PICO ECL substrate onto a chemiluminescent film.

Fluorescence Microscopy: HEK-293T cells were grown in DMEM supplemented with 10% FBS and 1% penicillin. Cells were transfected with GFP-vector, KATE-vector, GFP-PCAF, and KATE-RASSF1A using JetPrime transfection reagents according to manufacturing protocol. Pictures were obtained with an Olympus fluorescent microscope.

DISCUSSION

Results from our experiments have revealed a way in which RASSF1A may mediate tumor suppression. Here we show a novel interaction between RASSF1A and PCAF that is regulated by Ras and that this interaction also regulates the PCAF-mediated acetylation of β -catenin. As acetylation of β -catenin is known to be an activating event, this serves as a novel mechanism by which RASSF1A can modulate this potent oncoprotein. Consequently, loss of RASSF1A leads to the aberrant acetylation and activation of β -catenin. An explanation for this phenomena may be that RASSF1A may serve as a scaffolding protein for PCAF and its targets, thereby focusing PCAF activity away from β -catenin when present. This is supported by the co-localization of both proteins in the cytoplasm accompanied with the decrease of PCAF nuclear speckles, as seen in the images obtained from fluorescence microscopy.

This novel discovery has profound implications and important clinical relevance, since Ras proteins are widely involved in many human cancers and RASSF1A is frequently inactivated. RASSF1A has many functions as a tumor suppressor protein, including the regulation of the cell cycle, stabilization of microtubules, and induction of apoptosis in the cell. Identifying one biological mechanism that RASSF1A may implore to suppress Ras-mediated transformations can be vital in cancer therapeutics. Future research should explore the biological significance of the Ras-regulated RASSF1A-PCAF interaction may have in the cell, and whether this significance can also be seen across members of the RASSF family.

ACKNOWLEDGEMENTS

I would like to thank the NCI R25 University of Louisville Cancer Education Program (R25CA134283) program. I would also like to acknowledge the following people: Dr. Lee Schmidt, Dr. Geoff Clark, Dr. Howard Donninger, Desmond Stewart, David Beyerle, and Zach Long for all their help, advice, and encouragement over the summer.

Exploring Concordance between Sputum Eosinophil Analysis and Fractional Exhaled Nitric Oxide in Older Adults with Asthma

Noela Botaka¹, Anna Jorayeva PhD², Barbara J. Polivka, PhD, RN², Bryan Beatty, RRT, CPFT³, Diane Endicott, RN²

¹ University of Louisville, ²University of Louisville School of Nursing, ³University of Louisville Division of Pulmonary, Critical Care, and Sleep Disorders Medicine

INTRODUCTION

- Asthma is a chronic condition marked by inflammation of the airways.
- Asthma affects about 8% of all adults ≥ 65 years of age⁹.
- Eosinophilic inflammation accounts for up to 50% of all asthma cases¹¹.
- Sputum eosinophilic cationic proteins (ECP) and fractional exhaled nitric oxide (FeNO) assess airway inflammation.
- There is no consensus in the literature regarding the optimal method of evaluating airway inflammation, especially for older adults with asthma.

OBJECTIVE

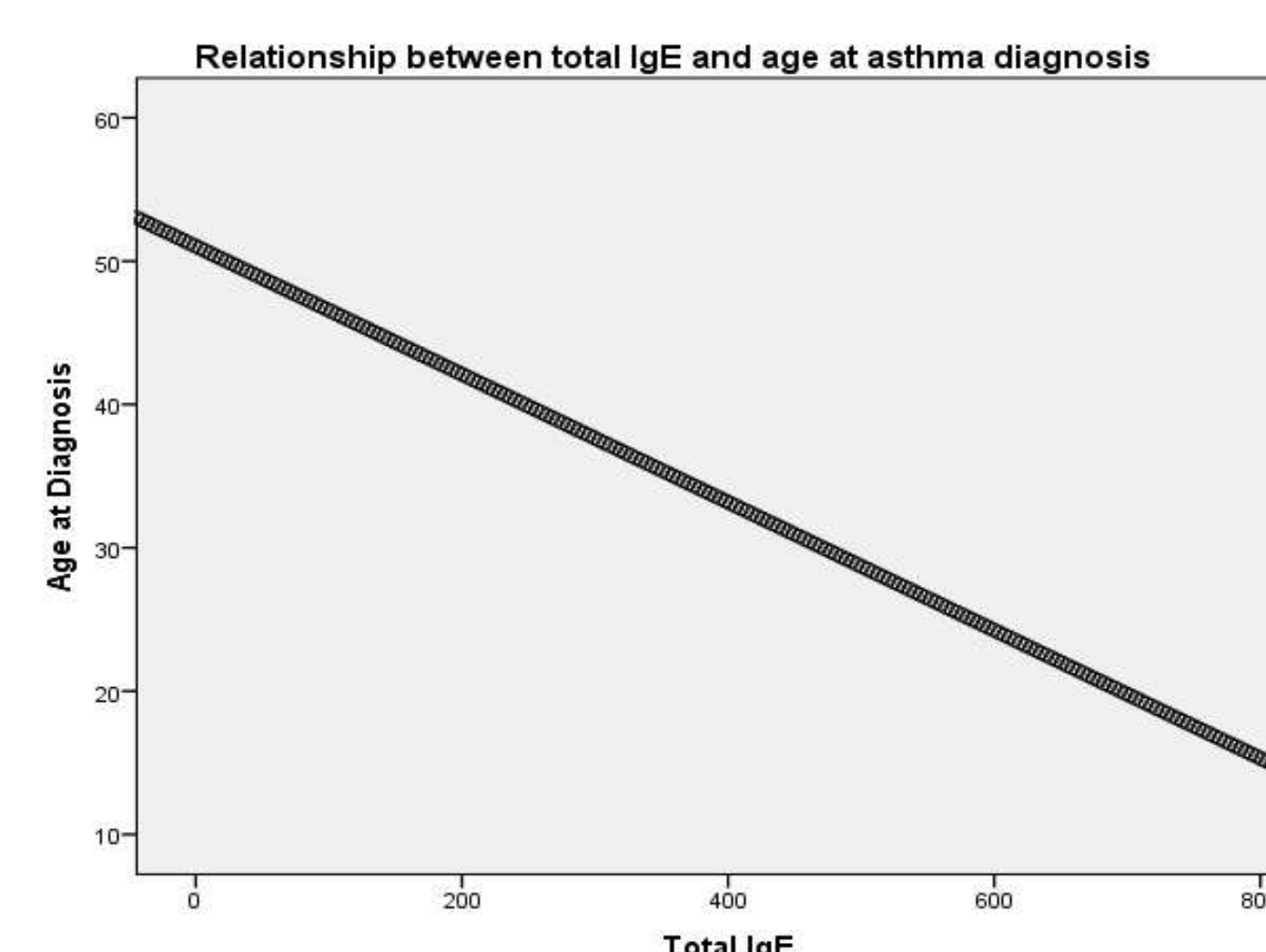
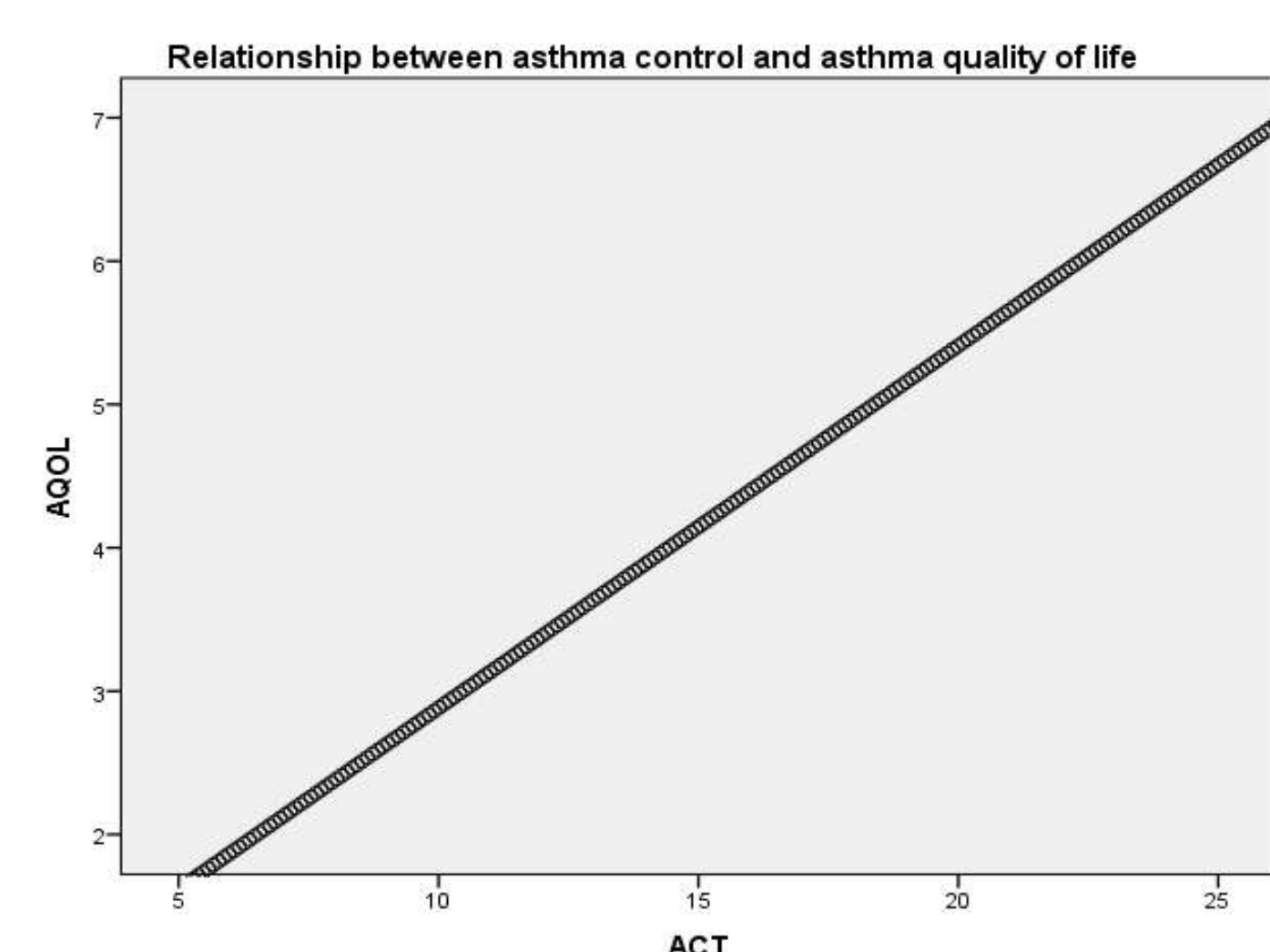
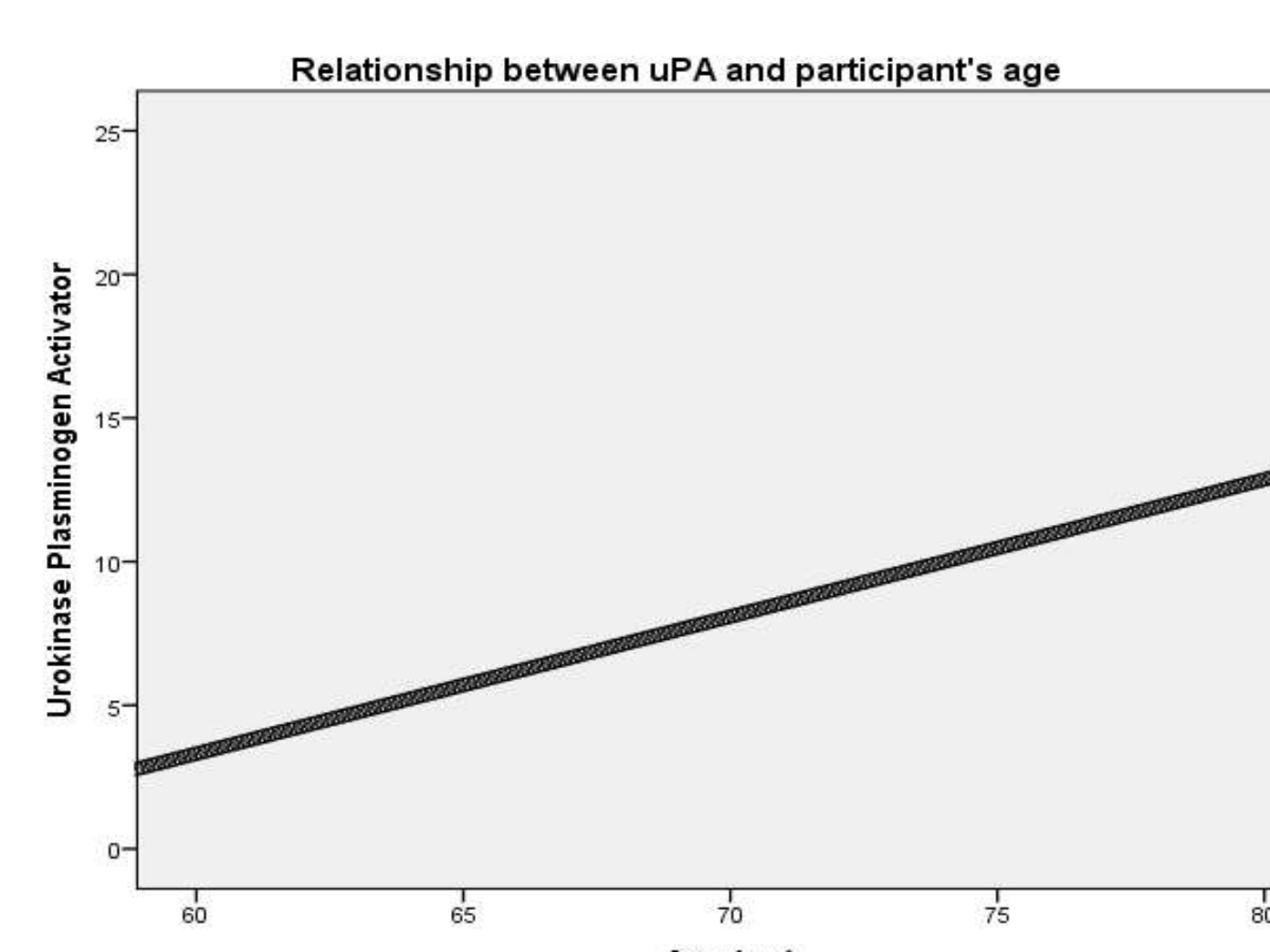
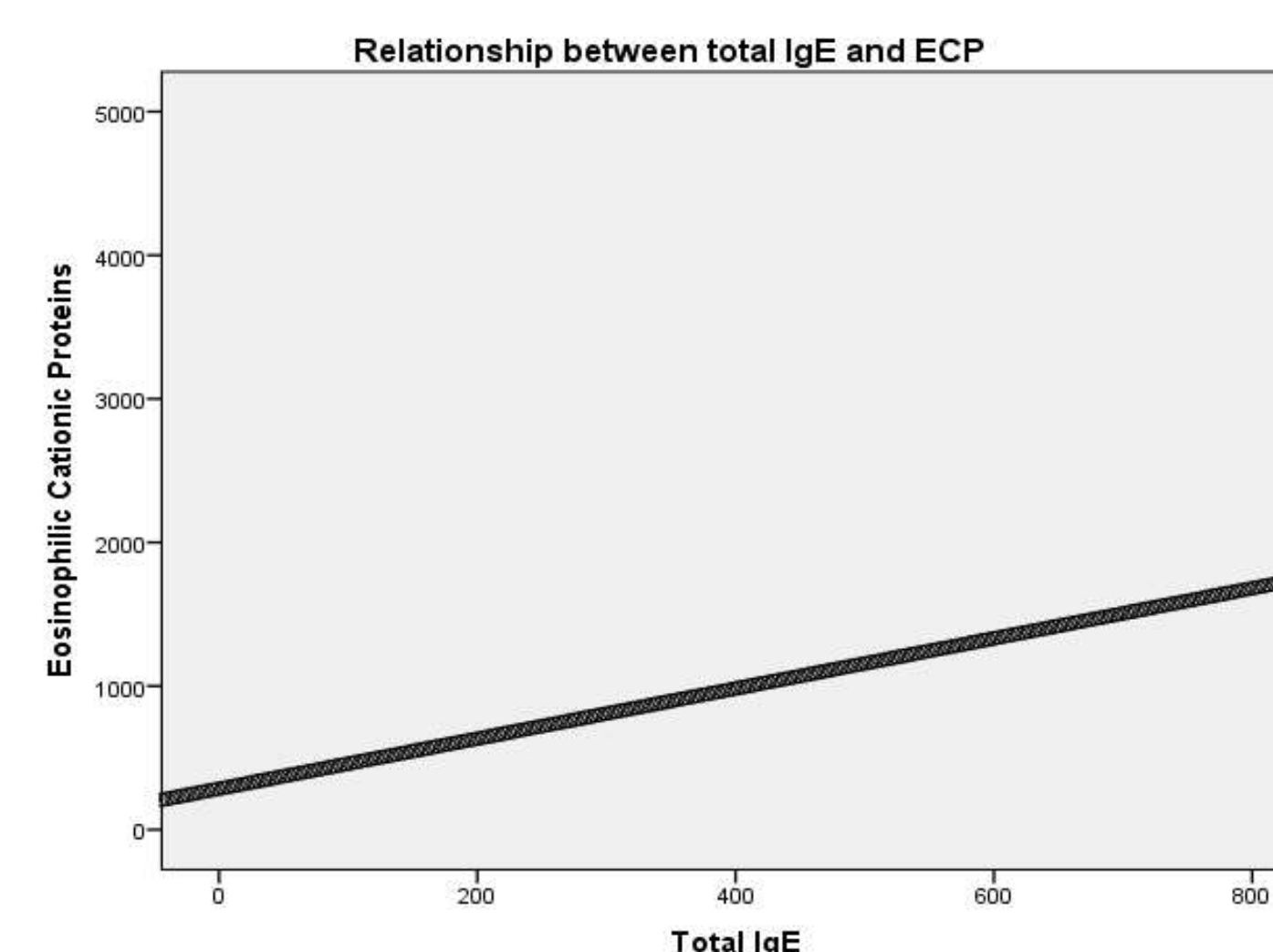
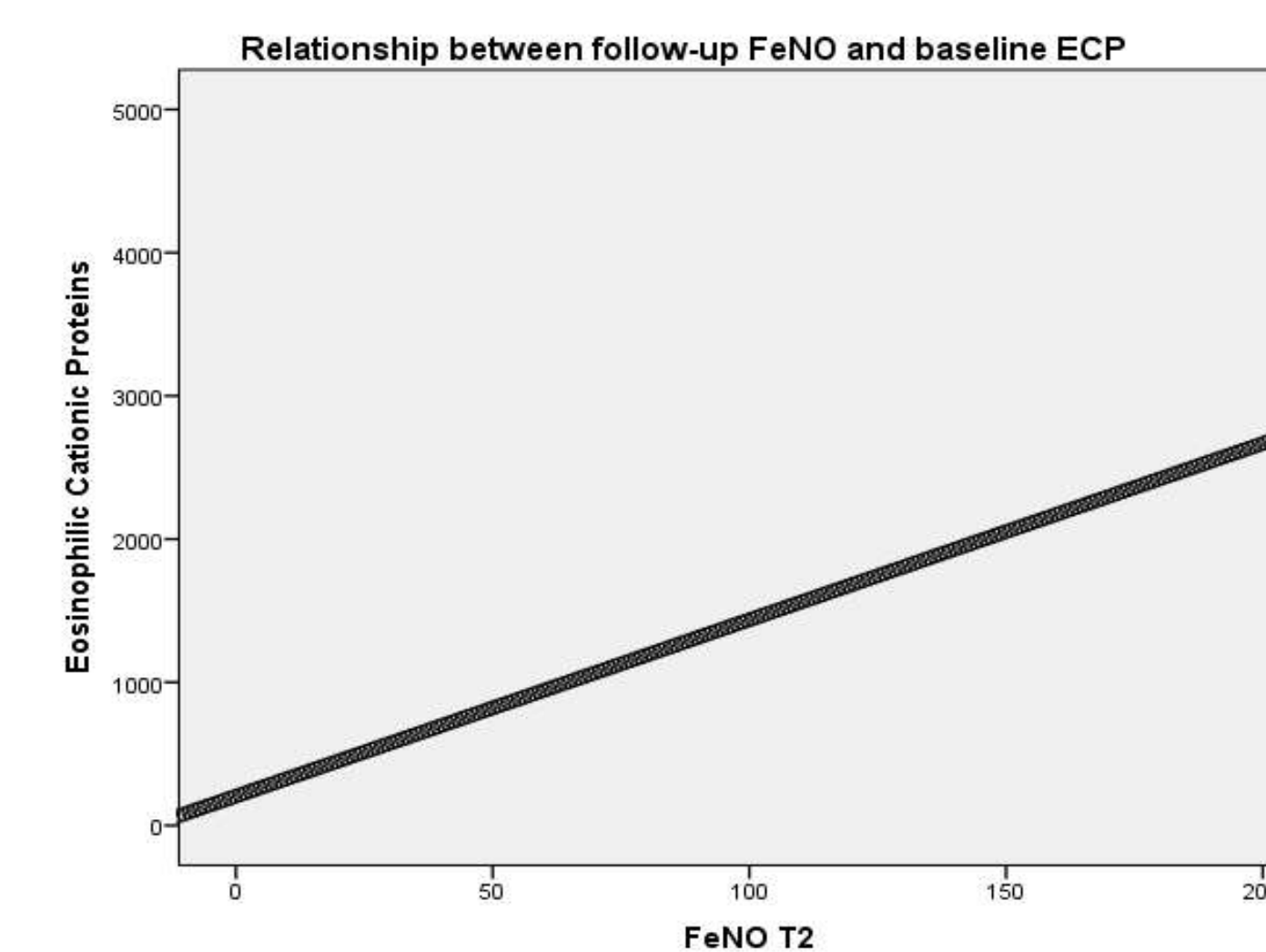
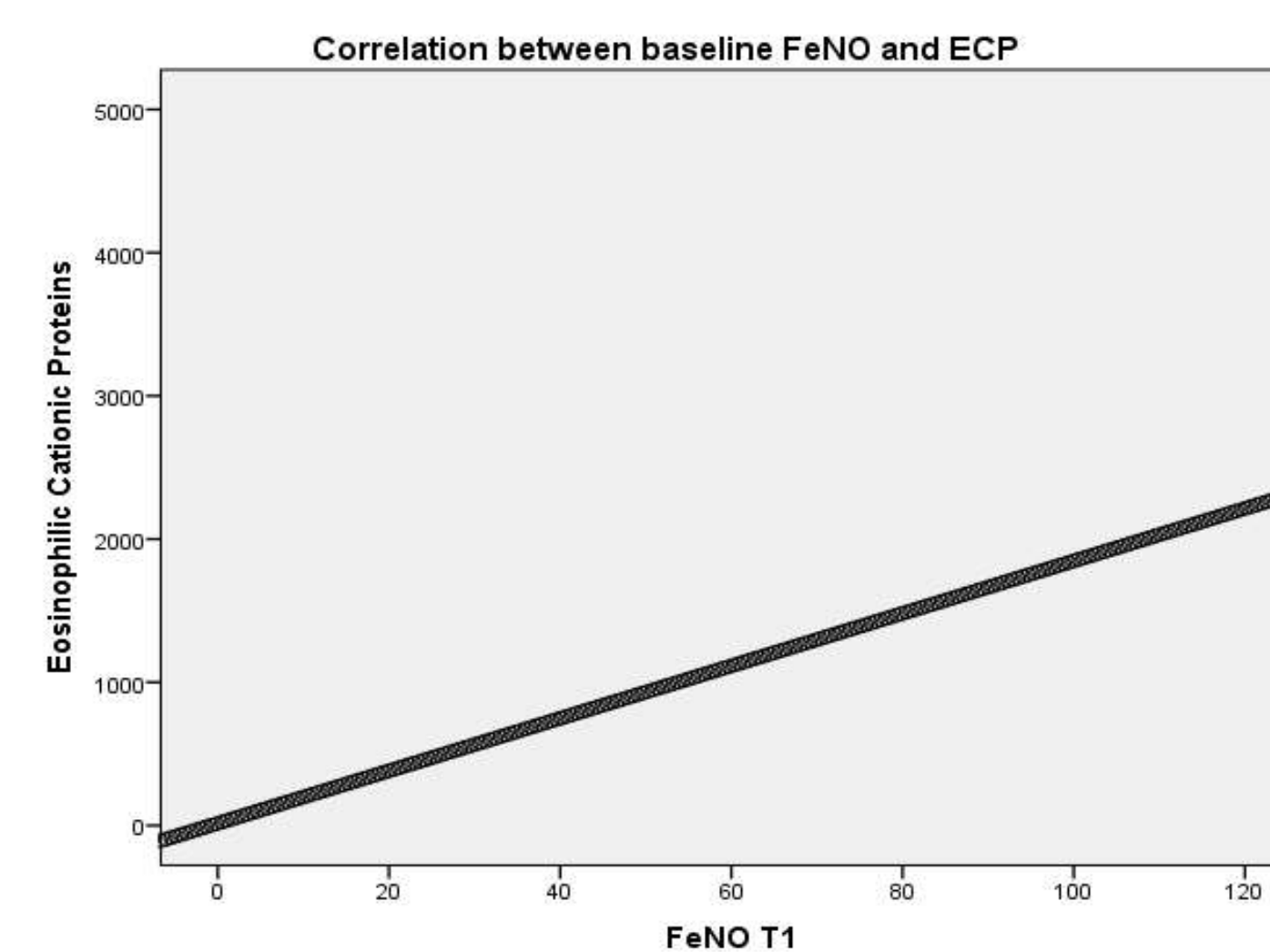
- The purpose of this study was to explore the concordance between FeNO and sputum eosinophil analysis in older adults with asthma.

METHODS

- Cross-sectional analysis of data collected during an ongoing, IRB-approved longitudinal study of older adults with asthma
- A subset of participants was used for this investigation ($n=29$, 83% Caucasian, 62.1% female, 67 ± 5 years old).
- FeNO was measured by NIOX VERO (ppb).
- Sputum was induced and analyzed for ECP.
- Blood samples were processed for immunoglobulin (IgE, U/ml) assays.
- Asthma management was assessed by asthma control (ACT) and asthma quality of life (AQLQ) using standardized self-report questionnaires.

RESULTS

- The average age at asthma diagnosis was $44 \text{ years} \pm 23$
- FeNO at baseline (T1) and at 9 months (T2) averaged 30 ± 26 and 29 ± 29 respectively, indicating moderate airway inflammation.
- Total IgE averaged $155.25 \text{ U/ml} (\pm 202)$, indicating present IgE-mediated allergic response.
- **A significant positive correlation** was found between
 - FeNO levels and sputum ECP ($r = .55, p < .01$) at baseline and at 9 months ($r = .41, p < .05$)
 - Total IgE and sputum ECP ($r = .40, p < .05$)
 - Urokinase Plasminogen Activator (uPA) and participant's age ($r = .59, p < .01$)
 - ACT and AQLQ ($r = .86, p < .01$)
- **A significant negative correlation** was found between
 - Total IgE and the age at diagnosis ($r = -.38, p < .05$)



DISCUSSION

- The findings of relationships between ECP and FeNO⁶ and AQLQ and ACT^{3,17} are consistent with other literature on adults with asthma.
- The positive relationship found between IgE and ECP may partially be due to IgE's role in eosinophil degranulation of ECP^{14,15}.
- The positive interaction found between the uPA and age may be related to the physiology of the aging process, decreased immune response, and increased inflammation⁴.
- The negative correlation between total IgE and age at diagnoses could be partially explained by immunosenescence^{2,7,8,18}.
- Major limitations of this exploratory study are small sample size and self-administered nature of the questionnaires.

CONCLUSIONS

- Evaluation of airway inflammation is critical in the diagnosis and management of asthma.
- Although not supported by the study results, inflammation can impact asthma control and quality of life^{3,18}.
- FeNO testing could be appropriate proxy for eosinophilic inflammation assessment in older adults with asthma.
- Future research should examine these relationships in a larger, more diverse sample and explore interaction between FeNO and ECP of patient groups stratified by inhaled corticosteroid treatment (ICS) modalities.
- If validated, FeNO could potentially serve as a clinical tool in lung cancer diagnosis and management, as FeNO devices are capable of adequately capturing pulmonary inflammation.

ACKNOWLEDGEMENTS

- Research reported in this presentation was supported by the National Institute on Aging under Award Number R01AG047297 and by the National Cancer Institute R25 CA-134283 Cancer Education Program Grant at the University of Louisville.

Introduction

G protein-coupled receptors (GPCRs) are encoded by a large family of genes and continue to be pursued avidly as major drug targets. It is estimated that 30-50% of the medicines currently available act either positively (agonists) or negatively (antagonists/inverse agonists) on GPCRs. G protein-coupled receptor 12 (GPR12) was first cloned from a mouse cDNA library in 1993 and was originally named GPCR21. This was followed by cloning of human GPR12, along with the two related orphan receptors GPR3 and GPR6, from a human genomic DNA library. In the brain, GPR12 receptor is located in the limbic system structures and to a lesser extent in the cerebral cortex, hippocampus, olfactory bulb, and striatum. Peripherally GPR12 is found in the testis and oocytes.

GPR12 has been shown to be relevant to cancer metastasis. It has been shown that silencing of GPR12 led to the reduction of phosphorylation and reorganization of keratin 8 (K8) filaments, which modulate the viscoelasticity of metastatic cancer cells. In contrast, GPR12 overexpression stimulated K8 phosphorylation and reorganization. These findings are indicative that GPR12 may be a potential target for creation of compounds that are able to adjust viscoelasticity of cancerous cells, thus preventing tumor metastasis.

GPR12 has been shown to be constitutively active and couples to both G_s and G_i proteins. However, GPR12 is an orphan receptor with no confirmed ligands. Initially, lysophospholipids sphingosine-1-phosphate (S1P) and shingosylphosphorylcholine (SPC) and were identified as ligands for GPR12. However, a later study was unable to confirm either S1P or SPC as ligand for GPR12.

Despite being orphans, GPR12 share about 35% amino acid sequence identity in the transmembrane regions with the CB1 and CB2 cannabinoid receptors. Therefore, it is considered a "cannabinoid receptor-like orphan GPCR".

Objectives

1. Test various classes of cannabinoids for their potential effects on GPR12 using a cAMP accumulation assay. Classes of cannabinoids which were tested include endocannabinoids, phytocannabinoids, and synthetic cannabinoids.
2. Examine the involvement of G proteins in the effects of cannabinoids on GPR12.

Results

Figure 1: Constitutive activity of GPR12

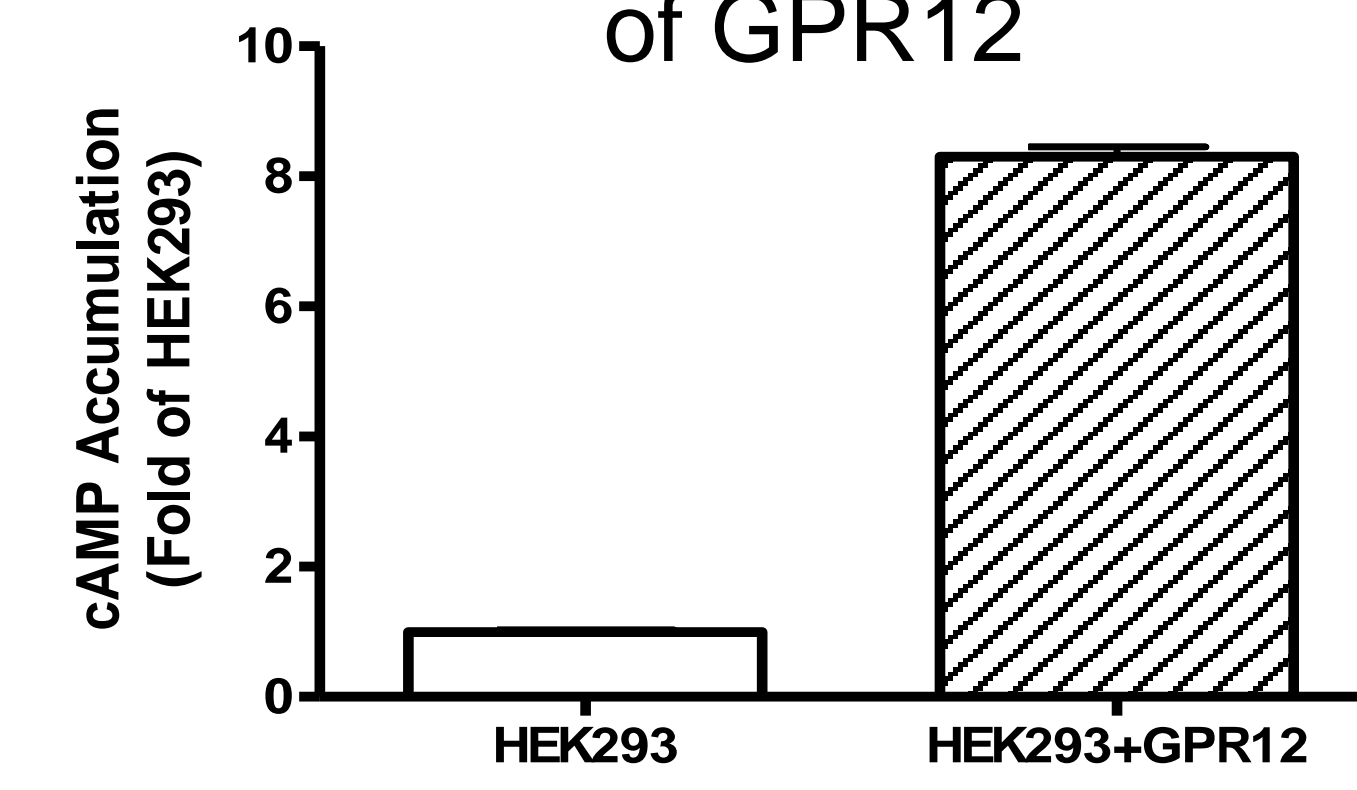


Figure 2: (cont.)

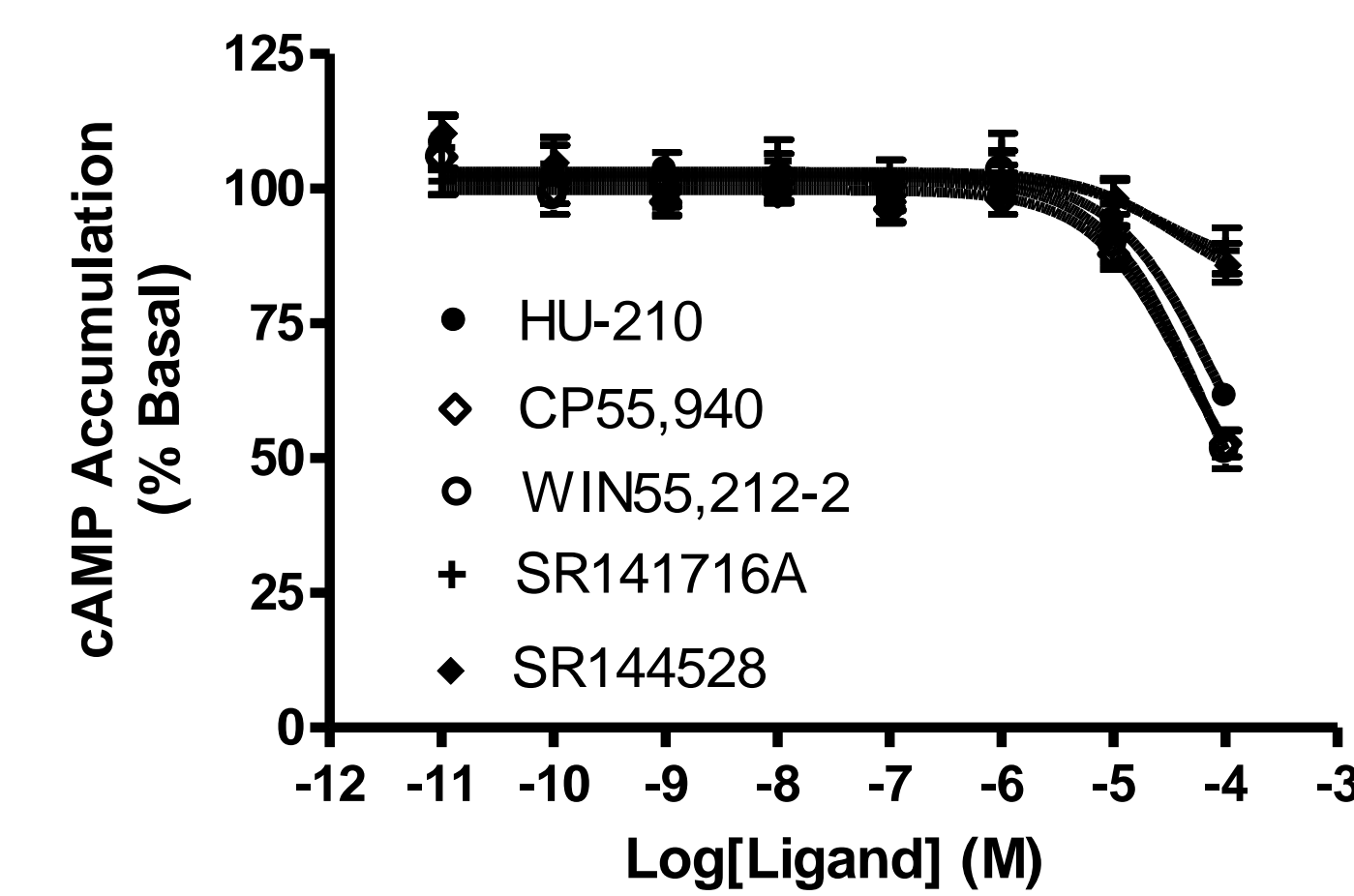


Figure 2: Effect of various classes of cannabinoids on GPR12-mediated cAMP accumulation

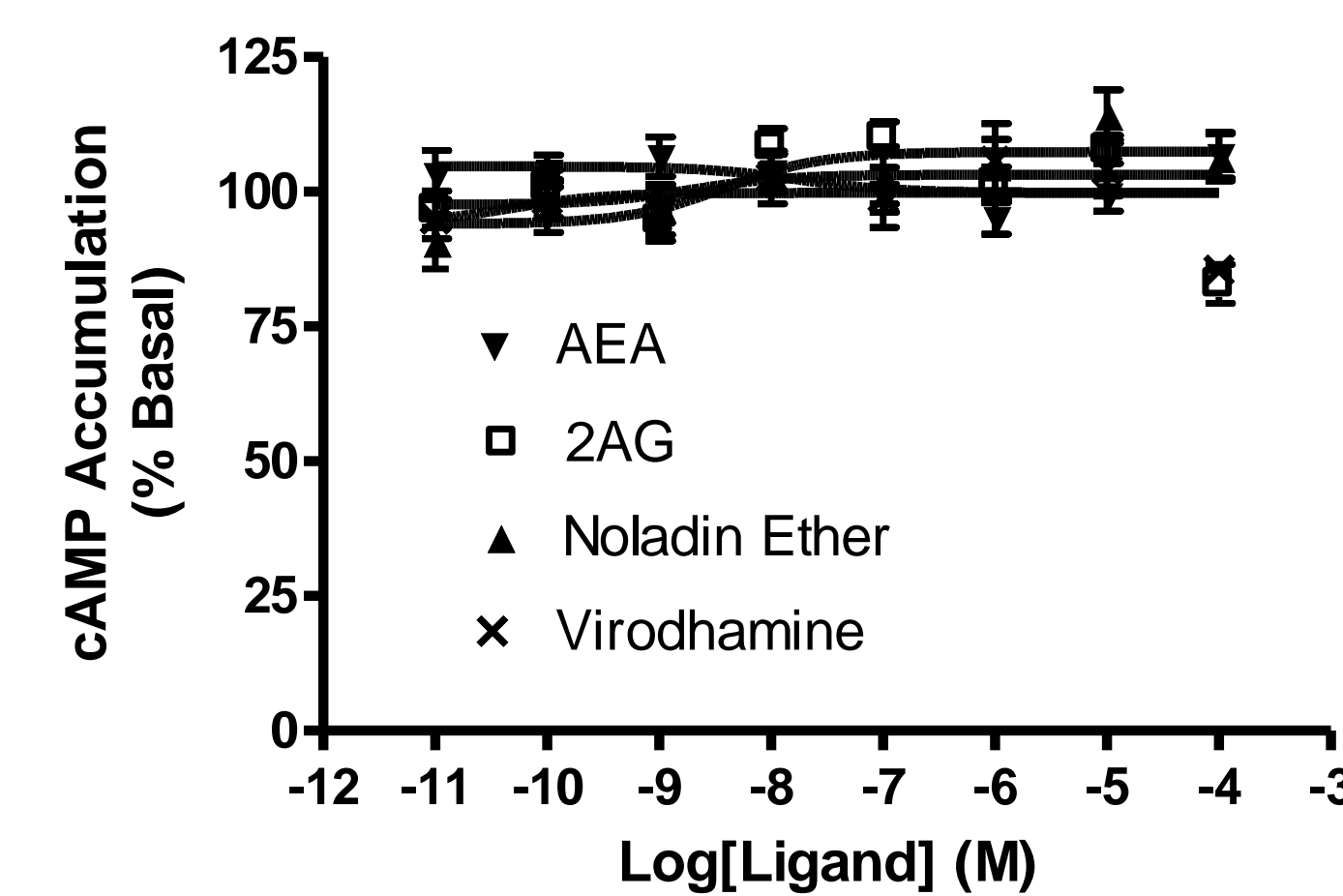


Figure 3: Structure-activity relationship of CBD on GPR12

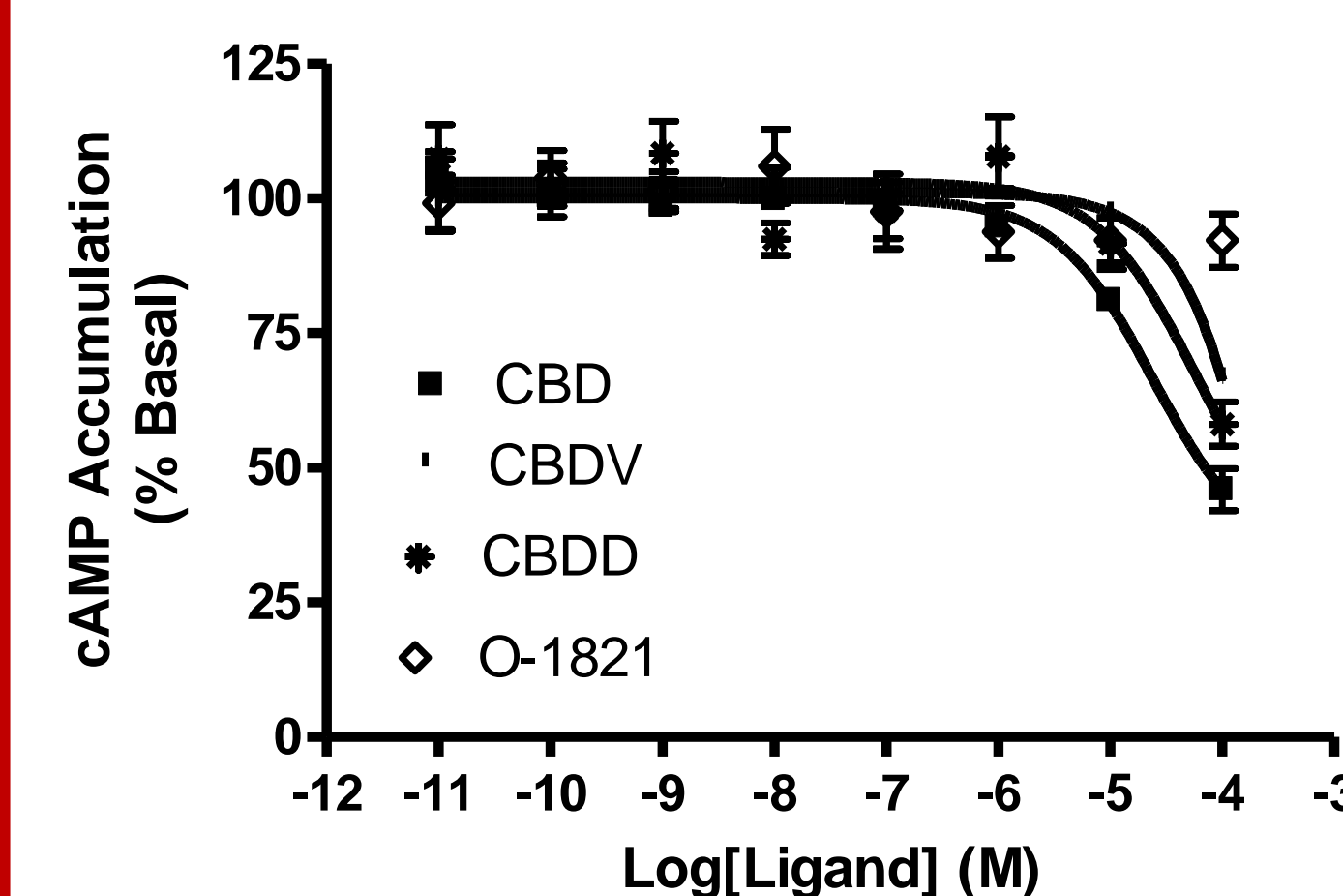


Figure 4: Comparison of WIN55,212-2 and WIN55,212-3 effects on GPR12

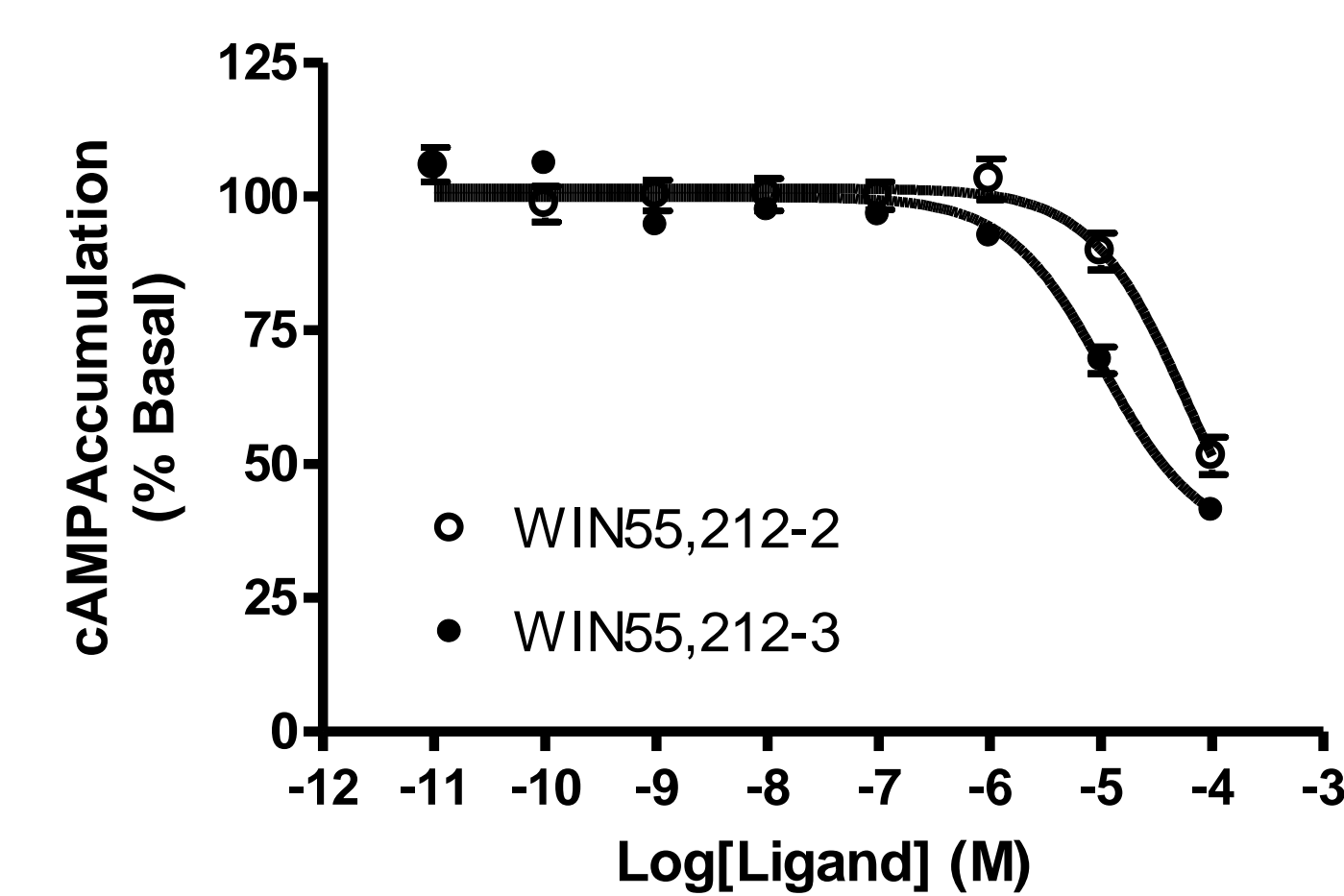
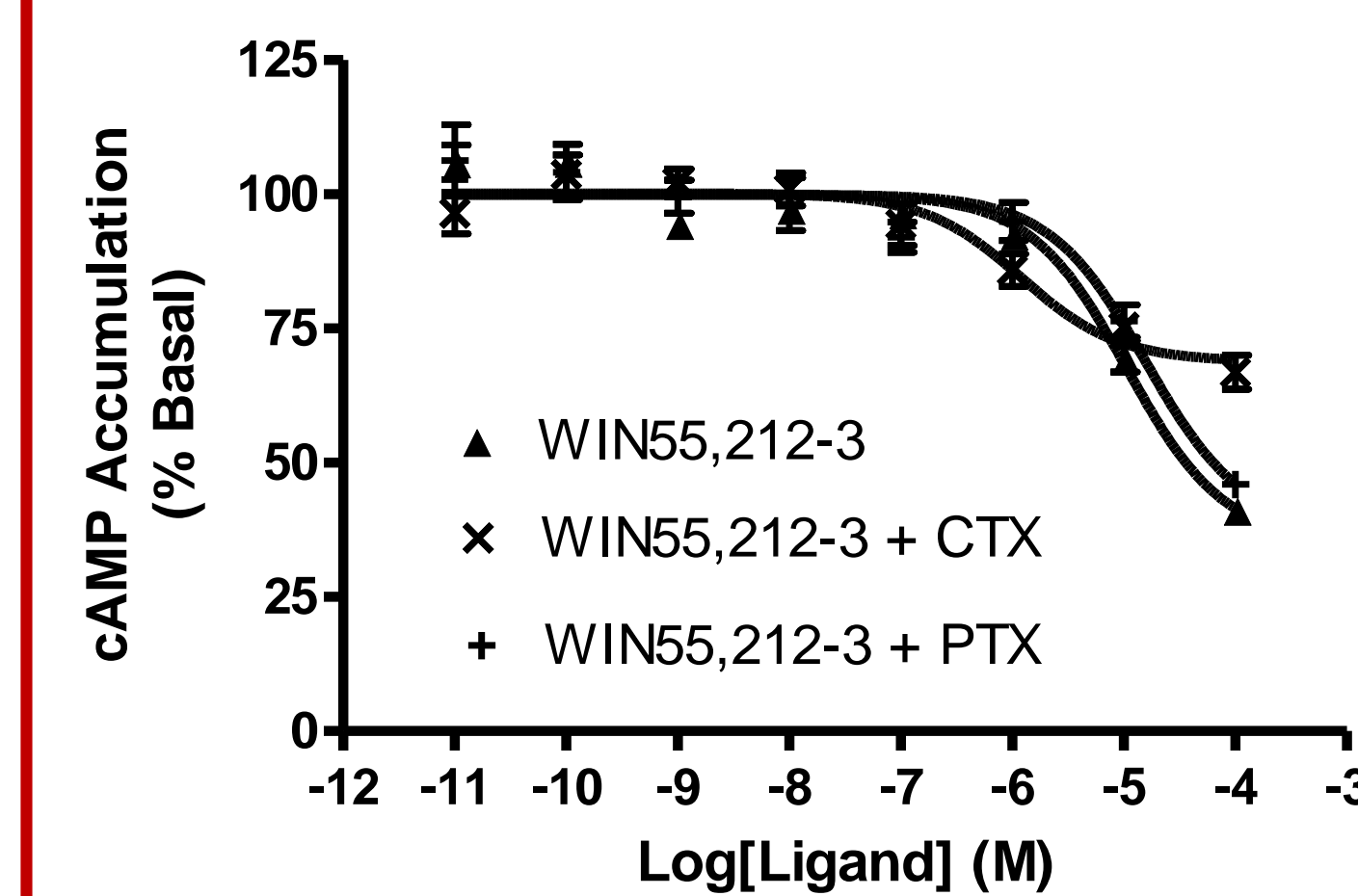
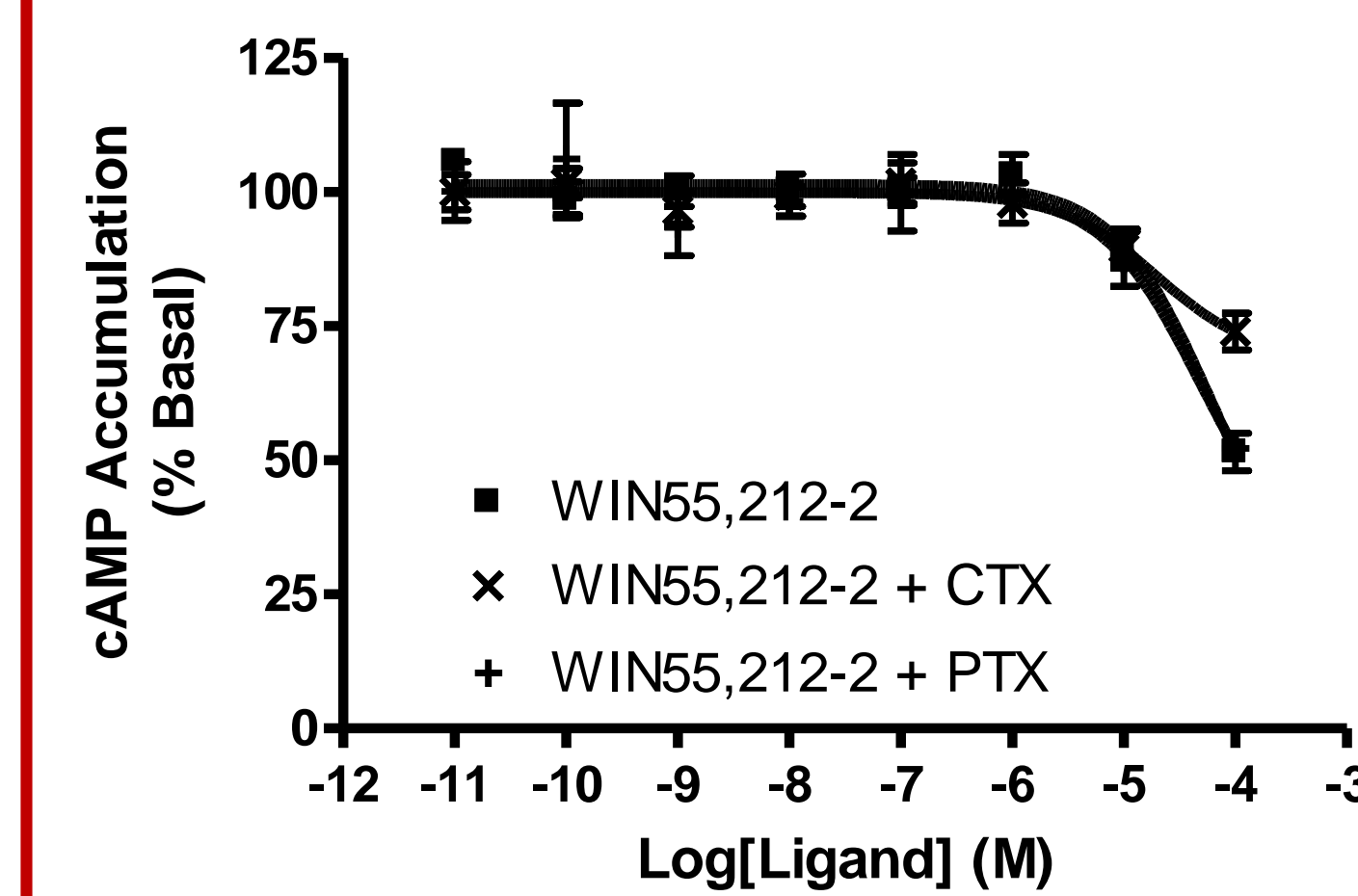
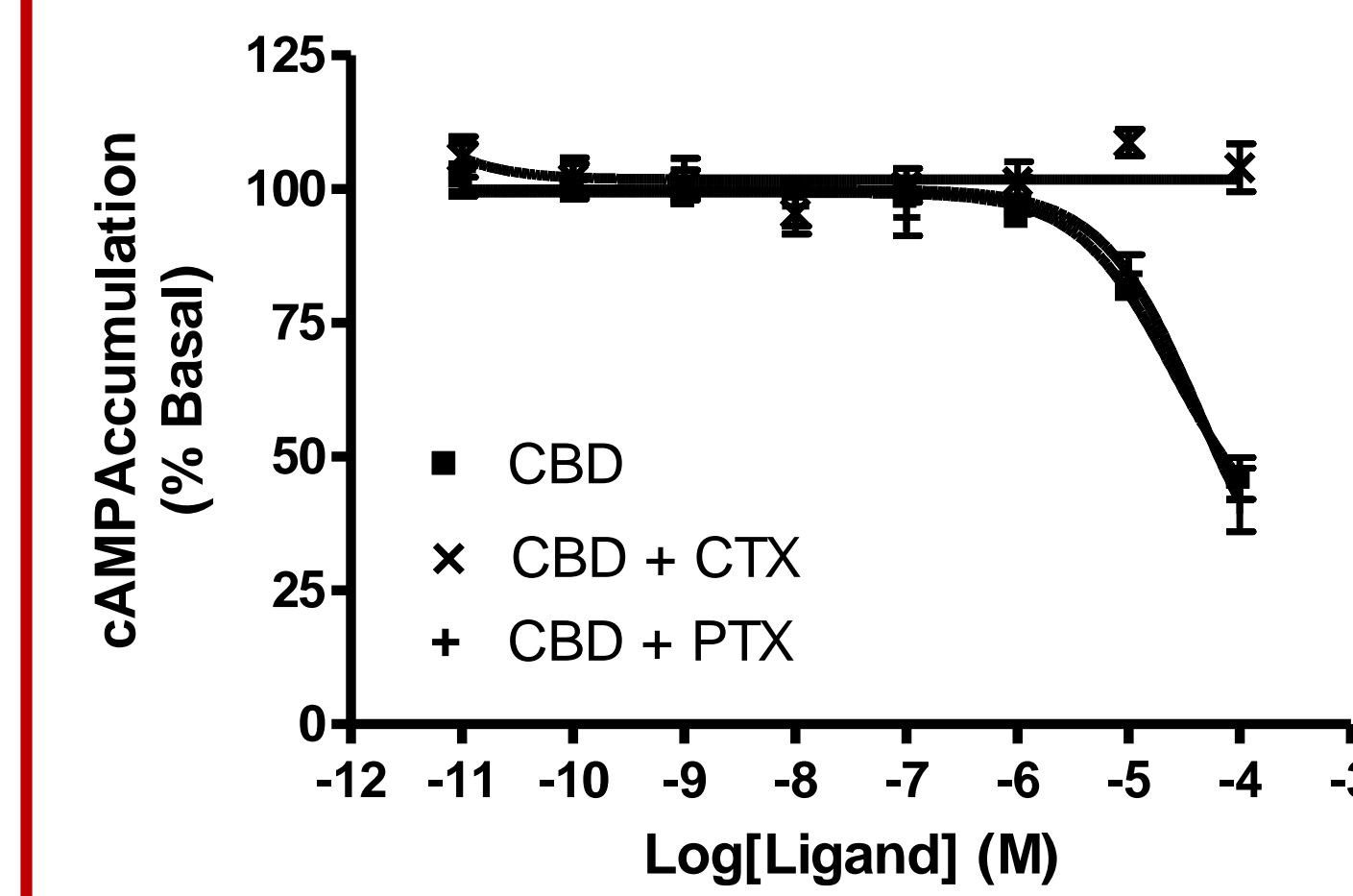


Figure 5: Involvement of G Protein in GPR12-mediated cAMP accumulation



Conclusions

1. GPR12 is constitutively activated.
2. None of the endocannabinoids significantly altered cAMP accumulation to GPR12. Among the phytocannabinoids, CBD and CBN significantly reduced cAMP accumulation to GPR12.
3. The free hydroxyl groups and the alkyl side chains are both important for the inverse agonistic effects of CBD.
4. WIN55,212-2 and WIN55,212-3 exhibit stereoselectivity at GPR12.
5. G_s proteins, but not G_i proteins, are involved in inverse agonistic activity of cannabinoids on GPR12.

Significance

The key finding of this study is that we have identified several cannabinoids to be inverse agonists of GPR12, a possible target for prevention of cancer metastasis. A previous study found that GPR12 may be involved in cancer metastasis by changing the migration of cancer cells. Since we have demonstrated that CBD, WIN55212-2 and WIN55212-3 are inverse agonists for GPR12, this provides the initial chemical scaffolds upon which highly potent and efficacious agents acting on GPR12 may be developed with the ultimate goal of preventing cancer metastasis.

Acknowledgements

This work is supported in part by the NCI R25 University of Louisville Cancer Education Program (R25-CA134283).

Effects of nasal deciliation on flavor preference: a model for chemotherapy-related chemosensory deficits

Brenda Dzaringa¹ and Chad L. Samuelsen²

¹University of Louisville Cancer Education Program Scholar

²Department of Anatomical Sciences and Neurobiology, University of Louisville School of Medicine, Louisville KY

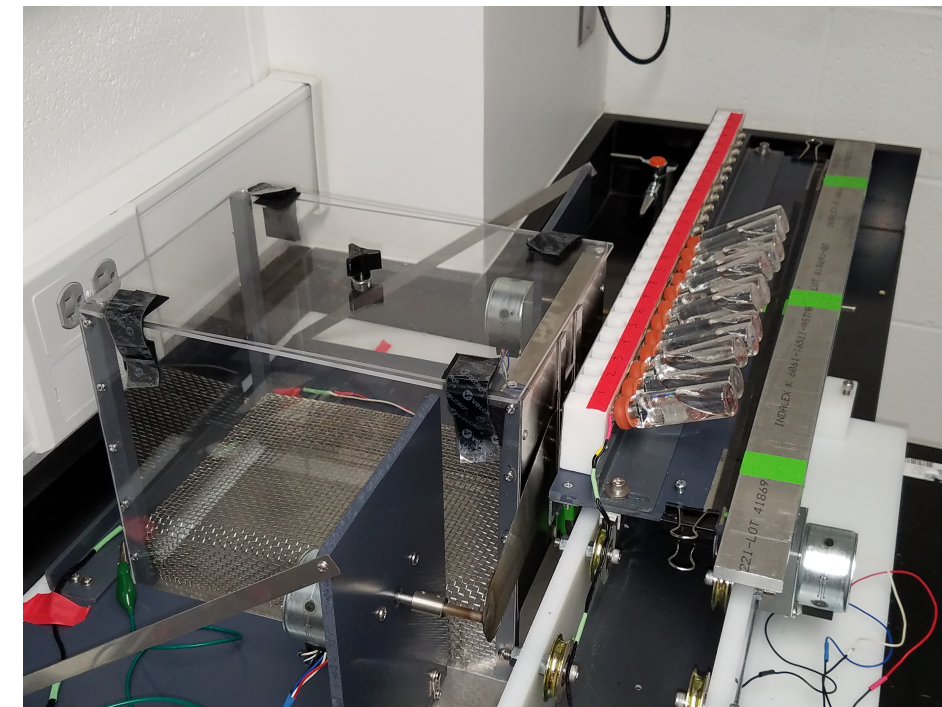


INTRODUCTION

The perception of flavor, the multimodal integration of the senses of taste and smell, is an essential element in choosing which foods to eat (Sclafani 2001). When placed in the mouth, food chemicals activate taste receptors on the tongue and travel retronasally to activate olfactory receptors in the nasal epithelium. Disruption of either the gustatory or olfactory system results in an altered perception of food. Approximately 70% of cancer patients report alterations of taste or smell (Hutton et al., 2007; Zabernigg et al., 2010) that can last for months to years after treatment (Mukherjee, et al., 2013). These deficits reduce the pleasantness of foods, leading to loss of appetite and weight loss (Boltong et al., 2012). This is a significant problem as malnutrition accounts for nearly 20% of cancer patient deaths (Silva et al., 2015). Using a custom built brief access two-bottle choice apparatus, we measure the preference for odors before and after disruption of olfaction by nasal deciliation. By perturbing olfactory function and examining odor preference, we provide a model for chemosensory deficits as a result of chemotherapy.

METHODS

TWO-BOTTLE APPARATUS



VIEW OF PORTS



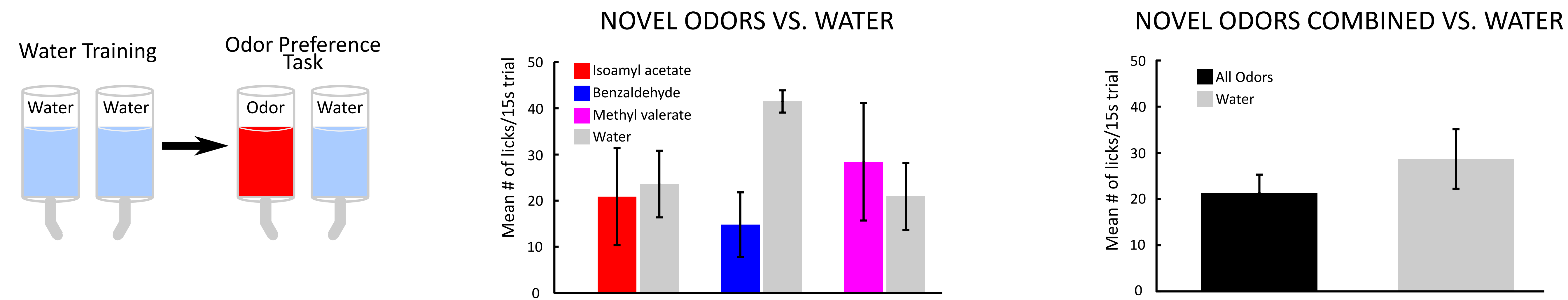
BEHAVIORAL PARADIGM

Two groups of female Long-Evans rats were placed on a water regulation schedule. All animals were habituated to the two-bottle apparatus by being placed in the test chamber and allowed to consume water from either port for 50 min., then to the opening and closing of the port doors and finally the movement of the bottle platform. Chemosensory training varied between the two experimental groups. One group was tested for preference of novel odors before flavor training. After this initial odor exposure, both groups of rats were given experience with flavors. One group received 10ml of odor paired with either 0.2M sucrose (IA, MV) or 0.2M citric acid (B). They other group had all odors (IA, B, and MV) paired with sucrose. After flavor training, rats were tested for IA, B and MV preferences versus water. Briefly, a rat would wait for 15s for the port doors to open. One port would contain water and the other an odor dissolved in water. Bottles were counterbalanced so that odors would be presented at both ports. Once open, the rat would have 15s to initiate a trial by licking either bottle. Upon contact with a lick spout, the rat received a further 15s to drink from the bottles. Every touch of the tongue completed a grounded circuit to register a lick. A session would last for 90 trials or 50 min. The average number of licks for odor and water were compared using 1-way ANOVA with tukey HSD correction. * p < 0.01.

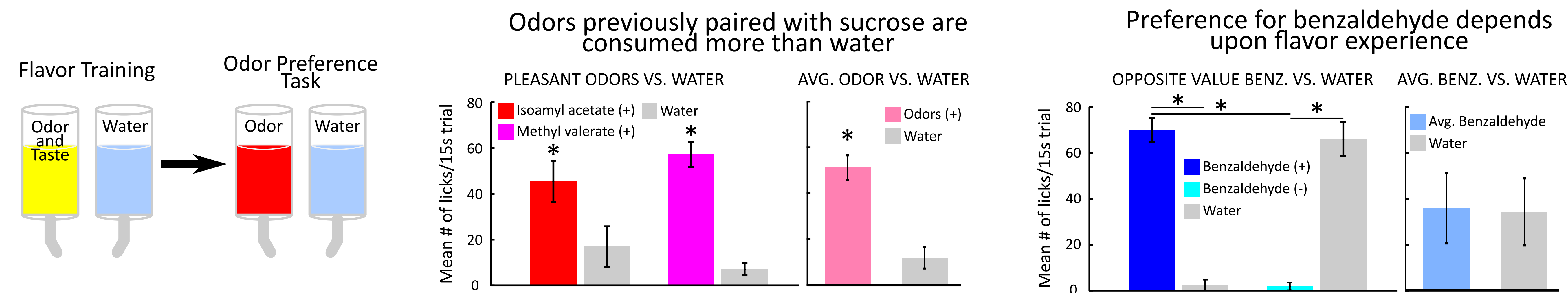
NASAL DECILIATION PROTOCOL

The nasal infusion protocol was the same regardless of treatment type (Triton X-100 or zinc sulfate). The day before testing the effect of nasal deciliation, 75 µl of a solution of 0.125% of Triton X-100 in 0.9% saline or 10% zinc sulfate was infused into one naris of an anesthetized rat and allowed 5 minutes before being removed by suction. The second naris was then treated in the same manner. Animals that had been tested for odor preferences prior to flavor training underwent three consecutive days of Triton X-100. The second group of animals received Triton X-100 every 2-3 days. Rats were tested for odor preferences as above.

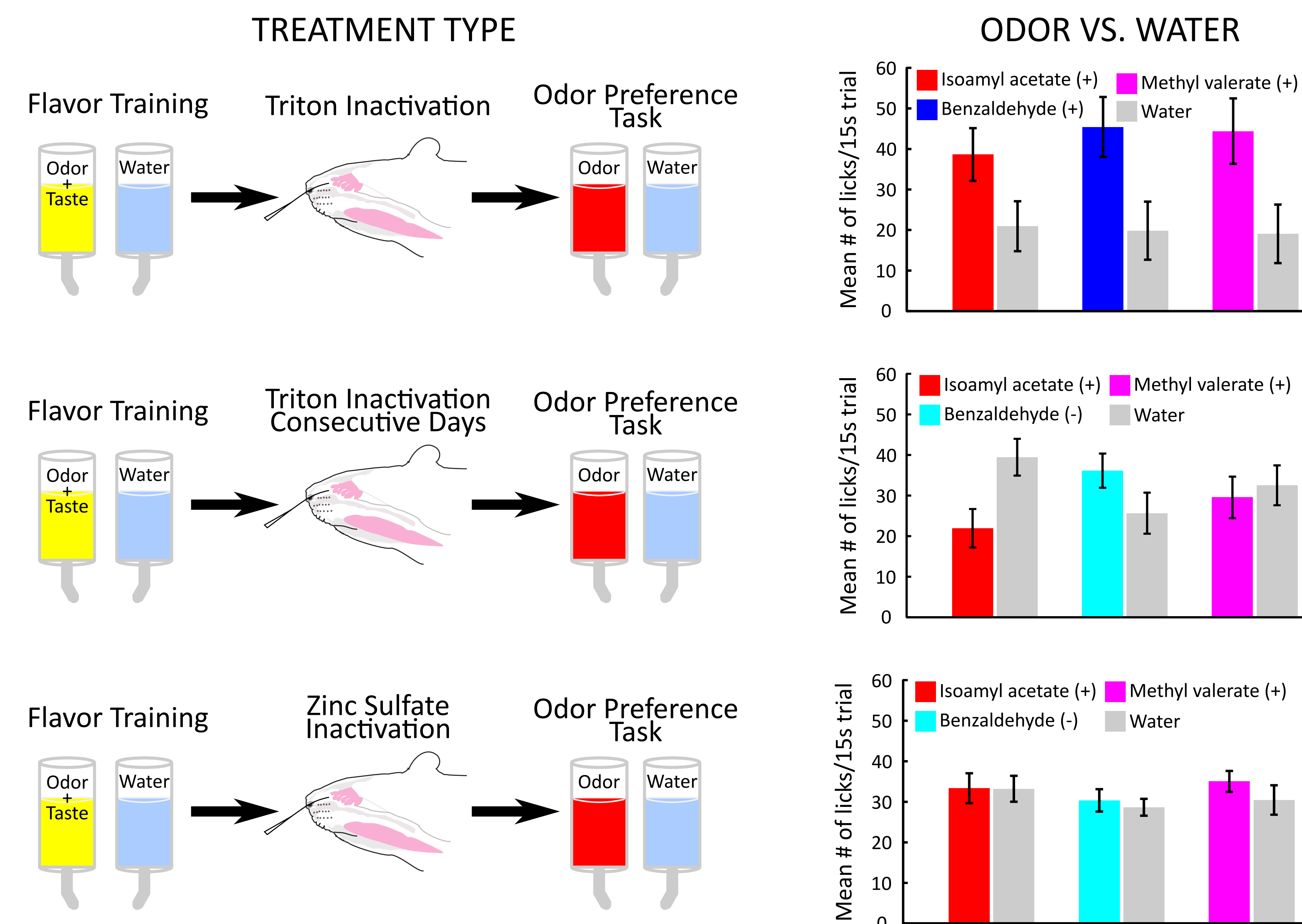
Prior to experience with flavors, odors are consumed similarly to water



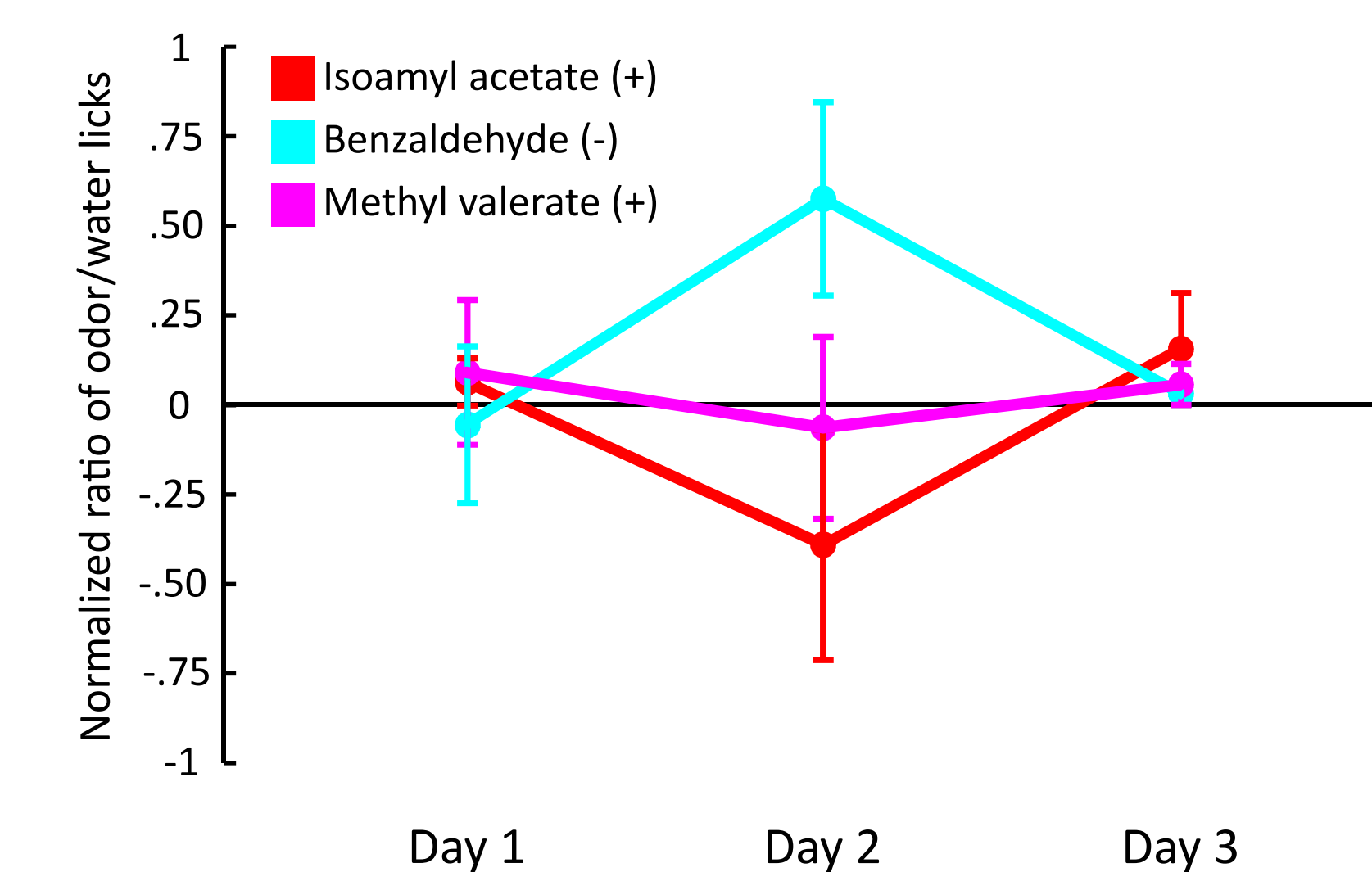
Flavor experience guides odor preferences



Nasal deciliation disrupts odor preferences



Nasal deciliation by consecutive Triton X-100 has long-term effects on odor preferences



SUMMARY

Without flavor experience, animals equally sample odor and water, indicating no preference for novel odors.

Sampling a flavor, the mixture of a taste and odor, links the affective value of a taste with the odor.

After experiencing flavors, odors previously paired with sucrose (IA, B, and MV) are consumed significantly more than water.

Animals that experienced a benzaldehyde-citric acid flavor pairing, consumed significantly less B than water.

Nasal inactivation by Triton X-100 and zinc sulfate disrupted olfactory function as measured by a brief access two-bottle odor preference task.

Nasal deciliation, by 3 consecutive days of Triton X-100 treatments, has long-term effects on olfactory function.

These findings confirm the brief access two-bottle preference task as a method to measure chemosensory preferences.

FUTURE DIRECTIONS

Chemotherapy treatments can alter the perception of both taste and smell. Chemotherapy drugs that inhibit sonic hedgehog signaling have little effect on olfactory morphology (Gong et al., 2009). However, taste buds are destroyed, greatly disturbing taste function (Kumari et al. 2014). We will use the sonic hedgehog inhibitor LDE225 (Kumari et al. 2014) to investigate how disruption of taste signaling alters learned odor preferences.

References

1. Belgaid K, Tishelman C, McGreevy J, Mansson-Brahme E, Orrevall Y, Wismer W, Bernhardt BM (2016) A longitudinal study of changing characteristics of self-reported taste and smell alterations in patients treated for lung cancer. *Eur J Oncol Nurs* 21:232-241.
2. Boltong A, Keast R, Aranda S (2012) Experiences and consequences of altered taste, flavour and food hedonics during chemotherapy treatment. *Support Care Cancer* 20:2765-2774.
3. Gong Q, Chen H, Farman AI (2009) Olfactory sensory axon growth and branching is influenced by sonic hedgehog. *Dev Dyn* 238:1768-1776.
4. Hutton JL, Baracos VE, Wismer W V (2007) Chemosensory Dysfunction is a Primary Factor in the Evolution of Declining Nutritional Status and Quality of Life in Patients With Advanced Cancer. *J Pain Symptom Manage* 33:156-165.
5. Kumari A, Ermilov AN, Allen BL, Bradley RM, Dlugosz AA, Mistretta CM (2015) Hedgehog pathway blockade with the cancer drug LDE225 disrupts taste organs and taste sensation. *J Neurophysiol* 113:1034-1040.
6. Mukherjee N, Carroll BL, Spees JL, Delay ER (2013) Pre-Treatment with Amifostine Protects against Cyclophosphamide-Induced Disruption of Taste in Mice. *PLoS One* 8.
7. Sclafani A (2001) Psychobiology of food preferences. *Nutr J* 14:123.
8. Silva FR de M, de Oliveira MGOA, Souza ASR, Figueroa JN, Santos CS (2015) Factors associated with malnutrition in hospitalized cancer patients: a cross-sectional study. *Nutr J* 14:123.
9. Zabernigg A, Gampfer E-M, Giesinger JM, Rumpold G, Kemmler G, Galttringer K, Sperner-Unterwiesing B, Holzner B (2010) Taste alterations in cancer patients receiving chemotherapy: a neglected side effect? *Oncologist* 15:913-920.

ACKNOWLEDGMENTS



This work has been supported in part by a grant from the National Cancer Institute R25 Cancer Education Program (BD; R25-CA134283) and the National Institute on Deafness and Other Communication Disorders (CLS; R03-DC0143198).